Westerduinweg 3
1755 LE Petten
P.O. Box 15
1755 ZG Petten
The Netherlands

www.tno.nl

T +31 88 866 50 65

TNO report

TNO 2018 R10850

Verification of ZephIR 300M unit 563 at ECN part of TNO LiDAR Calibration Facility, for offshore measurements at K13-A production platform

Date	April 2019
Author(s)	D.A.J. Wouters and J.P. Verhoef
Copy no	
No. of copies	
Number of pages	64 (incl. appendices)
Number of appendices	2
Sponsor	Dutch ministry of Economic Affairs
Project name	2018 Wind conditions @ North Sea
Project number	060.33997

Since April 1st, 2018 ECN and TNO have joined forces.

Management Summary

Title	:	Verification of ZephIR 300M unit 563 at ECN part of TNO LiDAR Calibration Facility, for offshore measurements at K13-A production platform
Author(s)	:	D.A.J. Wouters and J.P. Verhoef
Date	:	April 2019
Order nr.	:	ECN beschikkingsbrief EZK, 2018
Report nr.	:	TNO 2018 R10850

Revision

Rev.	Date	Description
0.1	07-2018	Initial draft
1.2	04-2019	Release

Archiving

\\tsn.tno.nl\RA-Data\Express\Wind-op-Zee

RvA is participant in the ILAC MRA.

ECN part of TNO Wind Energy is accredited conform ISO / IEC 17025 and accepted as RETL under IECRE WE-OMC.

- Power performance measurements according to IEC 61400-12-1, Measnet Power Performance measurement procedure, FGW TR2, FGW TR5
- NTF/NPC measurements according to IEC 61400-12-2
- Mechanical loads measurements according to IEC 61400-13
- Meteorological parameters (windspeed, wind direction, temperature, air pressure, relative humidity conform IEC 61400-12-1)
- Characterization of Remote Sensing Devices conform IEC 61400-12-1, Appendix L

Results only apply for the tested LiDAR with the settings used during the measurement period.
In case copies of this report are made, only integral copying is allowed.

Summary

As part of the North Sea offshore wind conditions measurement program a ZephIR LiDAR is installed at K13-A production platform on November 2016. In order to assure high quality measurements, the LiDAR unit (ZephIR 300M, 563) was validated at the ECN part of TNO LiDAR Calibration Facility for the period of 31 August 2016 00:00 until 10 October 2016 00:00. ECN part of TNO is ISO 17025 accredited for remote sensing device calibration, where the Meteorological Mast 4 measurements are in accordance with IEC 61400-12-1:2015, Annex G and the LiDAR verification in accordance with IEC 61400-12-1:2017, Annex L. The validation is performed by checking Key Performance Indicators.

The comparison of the LiDAR against the Meteorological Mast 4 is performed for 5 measurement heights: 29 m, 44 m, 59 m, 90 m and 100 m and the results for the validation and verification analyses are summarized in the tables below (see also tables 1 and 3).

KPI	height	result	unit	lower limit	upper limit	status
	m	unit		unit	unit	
$\text{slope}_{\text{WS},1p}$	100	0.985	-	0.98	1.02	pass
	90	0.997	-			pass
	59	0.991	-			pass
	44	0.997	-			pass
	29	0.994	-			pass
$R^2_{\text{WS},1p}$	100	1.000	-	0.98		pass
	90	1.000	-			pass
	59	1.000	-			pass
	44	1.000	-			pass
	29	1.000	-			pass
$\text{offset}_{\text{WD,median}}$	100	-1.987	°	-5	5	pass
	90	-1.840	°			pass
	59	-2.612	°			pass
	44	-1.280	°			pass
	29	-3.475	°			pass
$\Delta_{90_{\text{WD}}}$	100	2.653	%		3	pass
	90	2.678	%			pass
	59	2.421	%			pass
	44	1.556	%			pass
	29	0.000	%			pass

height	slope	offset	R^2
m	-	m/s	-
100	0.985	-0.003	1.000
90	1.002	-0.056	1.000
59	0.990	0.011	1.000
44	1.007	-0.100	1.000
29	0.983	0.096	1.000

A sensitivity analysis is performed for the LiDAR. Significant sensitivities were found for the environmental variable: relative humidity and wind direction. The results are shown in the table below (see also table 14). Relative humidity has the highest influence on the accuracy.

environmental variable	comparison height					overall
	100 m	90 m	59 m	44 m	29 m	
shear exponent						
turbulence intensity						
precipitation						
wind direction			✓			✓
air temperature						
relative humidity	✓	✓	✓			✓
air density						
flow inclination						
wind veer						
reference wind speed						

Based on these results ECN part of TNO qualifies this LiDAR unit as suitable for offshore application at the K13-A production platform.

Contents

List of tables and figures

Tables

Figures

1 Introduction

The Dutch government has ambitious plans for offshore wind energy towards 2020 and beyond. In order to achieve the goals that have been set, various development zones have been defined in the North Sea. The Dutch government creates a level playing field for developers among others to provide them with wind data on which business cases can be build.

To acquire wind data, the Dutch ministry of Economic Affairs has contracted ECN Wind Energy to carry out a measurement campaign on the North Sea. This campaign comprises among others of LiDAR measurements at Lichteiland Goeree (LEG), Euro Platform (EPL) and K13-A. To this end, the ZephIR 300M LiDAR 563 was installed at K13-A on November 2016.

High quality measurements will reduce the uncertainty in the measurements creating more favourable finance conditions for developers. Therefore, and to assure the high quality, the LiDAR was first verified and validated at the ECN part of TNO LiDAR Calibration Facility (ELCF) [1] located at the ECN Wind Turbine test site Wieringermeer (EWTW).

This report describes the comparison of the LiDAR with Meteorological Mast 4 (MM4) for the period of 31 August 2016 00:00 until 10 October 2016 00:00. The measurements at the mast are performed in accordance with IEC 61400-12-1:2005 [2]. Furthermore, the LiDAR is validated and verified, where validated means that Key Performance Indicators (KPIs) are checked. These KPIs are set up by ECN part of TNO based on NORSEWinD criteria [3] and the 'Carbon Trust Offshore Wind Accelerator roadmap for the commercial acceptance of floating LIDAR technology' [4]; they are defined in chapter 4. The verification is done in accordance with Annex L of IEC 61400-12-1:2017 [5].

The measurement campaign is described in chapter 2 and details the site, the mast and the LiDAR. It focuses on Meteorological Mast 4; a full description of the calibration facility can be found in the instrumentation report [1]. Chapter 3 describes the data preparation steps. The validation of the KPI's is discussed in chapter 4 and the verification analysis results are presented in chapter 5. In addition, a sensitivity analysis is presented in chapter 6. Chapters 7 and 8 present the uncertainty analysis and deviations with respect to the standards applied.

2 Measurement campaign

2.1 ECN part of TNO LiDAR Calibration Facility

The ECN part of TNO LiDAR Calibration Facility (ELCF) is part of the ECN Wind Turbine test site Wieringermeer (EWTW). The site mainly consists of agricultural land, with single farmhouses and rows of trees as shown in fig. 1. It is located in the Wieringermeer, a polder in the north east of the province of North Holland, 3 km north of the village of Medemblik. To the east, the site is 1 km removed from the vast lake IJsselmeer. The altitude is 5 m below sea level. The site is considered flat terrain according to IEC 61400-12-1:2017 [5].

Source: Google Maps

Figure 1: Overview of the EWTW; highlighted in red is the location of the ECN LiDAR Calibration Facility

2.2 Meteorological mast

The ELCF is detailed in a separate report [1]. The Meteorological Mast 4 is an essential part of the ELCF. It is a 100 m tall lattice tower with a triangular cross section, supported by guy wires at two levels: 41 m and 83 m. The guy wires are fixed to concrete anchors at a radius of 60 m from the tower base at 95°, 215° and 335°.

The MM4 and its sensors are detailed in appendix B. The wind speed is measured at 29 m, 44 m, 59 m, 90 m and 100 m. These are the heights at which the LiDAR measurements are compared to the MM4. The comparison heights are detailed in table 18.

At the heights of 87.5 m and 42 m multiple sensors are installed on two or three booms of MM4. By combining the signals from these sensors, the influence of the mast on the measurements can be minimized. The resulting signal is an example of what is referred to as a ‘pseudo signal’. All pseudo signals are defined in table 21. At 100 m two closely spaced anemometers are mounted accompanied by two vanes at 97 m. At 87.5 m two booms are installed, which measure the wind speed at 90 m and the wind direction at 88 m. At 42 m three booms are installed, which measure the wind speed at 44 m and the wind direction at 42 m. The layout of MM4 is shown in fig. 28.

All wind speed measurements are performed with Thies First Class Advanced cup anemometers. All wind direction measurements use Thies First Class wind vanes. The full instrumentation applicable for this report is listed in table 19. The sensors and data acquisition modules used are detailed in table 20.

The cup anemometers and wind vanes on MM4 are calibrated on a yearly basis, i.e. one year after the installation date. All instruments and data acquisition modules are calibrated according to internal procedures. Calibration certificates are available at the ECN offices in Petten. The latest calibration certificates of one of the topmost cups and vanes used are presented in appendix B.

2.3 LiDAR

The LiDAR is a ZephIR 300M. This unit has identification number 563. Using Waltz 4.60 with the ZPH files produced by the LiDAR, its firmware version is found to be 2.1027. According to the LiDAR configuration extracted from the CSV files, produced from the ZPH files using Waltz, the LiDAR (shown below), it is configured to perform measurements at ten heights: 29 m, 44 m, 59 m, 90 m, 100 m, 120 m, 140 m, 160 m, 180 m and 200 m. Note that the configured measurement heights are meaured above the ZephIR window, which is 1 m above the ground. The measurement height of 38 m above the lens is a default, non-configurable measurement height. The LiDAR has a cone half-angle of 30.0°. A picture of the ZephIR 300M LiDAR deployed at the ECN part of TNO LiDAR Calibration Facility during the verificiation test is presented in fig. 2. Figure 3 shows the LiDAR being deployed at K13-A.

Configuration of the LiDAR

```
CSV Converter: v1.209
Filter: v1.040
File system version: v4
Unit: 563
Time sync: UTC +0 hrs
38m is a fixed reference measurement
The GPS field contains latitude and longitude coordinates in decimal degrees (positive sign indicates North or East)
ZephIR window height above ground: 1.0m
Measurement heights: 199m 179m 159m 139m 119m 99m 89m 58m 43m 38m 28m
```

To achieve the highest quality LiDAR measurements, a filter named ‘availability’ is defined based on the number of packets logged for each 10-minute averaged sample. In order to quantify the overall availability of the LiDAR in a 10-minute interval (for a certain height), we normalize the number of packets in a 10-minute interval to 100 % using

$$\text{availability} = \frac{n_{\text{packets}}}{\max(n_{\text{packets}})} \cdot 100\,\% \tag{2.1}$$

where $\max(n_{\text{packets}})$ is the maximum (common) value for the number of packets metric observed in the entire data set.

Photo by Carel van Diggelen

Figure 2: ZephIR 300M, unit 563, indicated in red, at the ECN part of TNO LiDAR Calibration Facility at the base of Meteorological Mast 4

Photo by Carel van Diggelen

Figure 3: ZephIR 300M, unit 563 being deployed at the K13-A production platform

2.4 Measurement sector

As part of the ELCF a dedicated platform for placing remote sensing equipment is created near the anchor of the 215° guy wires. However, at the start of this campaign the infrastructure for the platform had not yet been completed. Therefore, the LiDAR was placed at the base of MM4, as shown in fig. 2. The area surrounding MM4 is very flat as demonstrated by the laser altimetry in fig. 4.

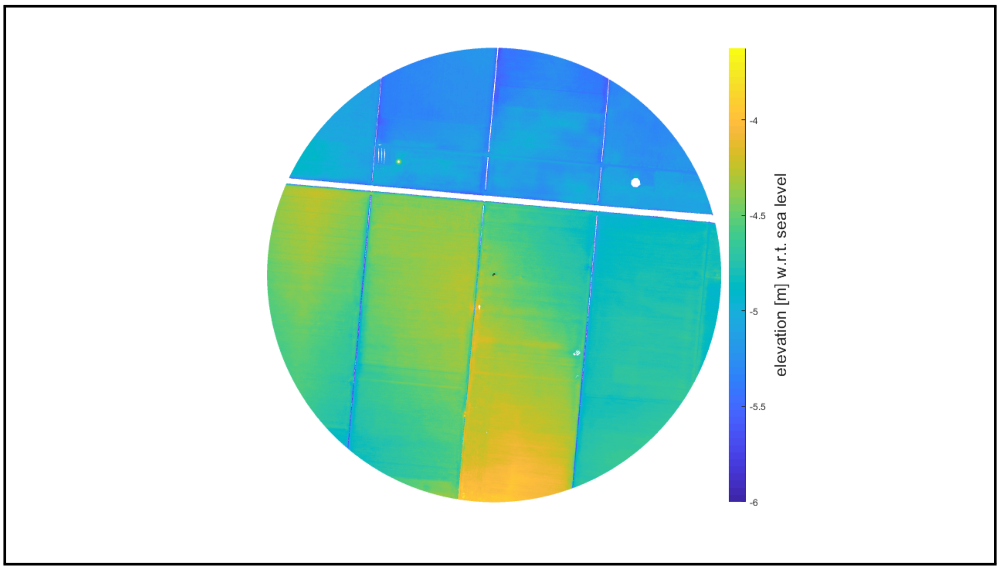

Source: PDOK / AHN-3 (0.5 m raster DTM)

Figure 4: Ground level elevation map of the LiDAR's surroundings (radius = 5 × 100 m)

The wind direction sector for which the measurements of both the mast and the LiDAR are unaffected by obstacles is referred to as the measurement sector. It is determined using Meassector 2.2.1 [6]. The objects affecting the measurement sector are shown in fig. 5. Figures 4 and 5 use the same grid map (RD-coordinates). All angles are relative to the grid North.

The total measurement sector is composed of the following sectors.

- 356.5° to 24.2°
- 104.5° to 284.1°

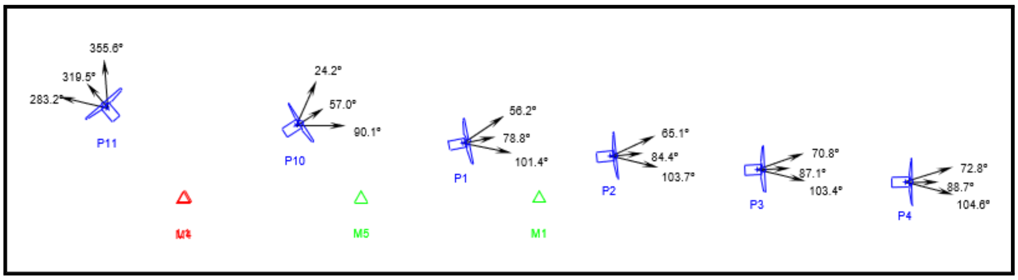

Source: Meassector 2.2.1

Figure 5: Measurement sector. Total excluded sector per obstacle. (In red, the closely spaced markers are *M4* for MM4 and *L1* for the LiDAR)

2.5 Data stream

The Meteorological Mast 4 is connected via a glass fibre network to the measurement office on the test site. From here, the data are transported on a daily basis to the offices in Petten, where they are stored in a dedicated Wind Data Management System (WDMS) database [7].

The LiDAR data are accumulated in the LiDAR device itself. The data files are transferred directly to the offices in Petten. The ZPH files are imported into the WDMS database.

Valid data are gathered from 31 August 2016 00:00 until 10 October 2016 00:00. All times are expressed in UTC.

3 Data preparation

The validation, verification and sensitivity analyses are performed using 10 minute average values. The following data filters are applied at each comparison height, in accordance with Annex L.2.3 [5].

a) Mast free of wake from obstacles
The measurement sector is defined in section 2.4 and the filtering is applied to the wind direction measurements at each comparison height individually.

b) LiDAR probe volumes free of wake from obstacles
The measurement sector ensures the LiDAR is not in the wake of any obstacles. However, the LiDAR could be affected by the wake of the MM4.

The LiDAR is located close to the base of MM4. For this analysis the probe volumes are represented by the entire conical measurement volume. At all measurement heights Meteorological Mast 4 is inside the (circular) measurement volume of the LiDAR. The potential interference of the wake of MM4 on the LiDAR, is visualised in fig. 24. These figures show the ratio of the wind speeds measured by MM4 and the LiDAR for each comparison height. We do not apply any filtering.

c) Anemometers free of wake from mast
The influence of the MM4 wake on the reference cup anemometers is mitigated by using multiple cups on booms at different angles at most measurement heights, combined with the pseudo signal equations listed in table 21. At comparison height 59 m only a single boom is present. In this case the additional sector of 310° to 360° is omitted for the wind speed measurements at this comparison height. The filtering performed is based on the wind direction measured by the wind vane installed at this comparison height. This filtering has no influence on the data, because the sector 310° to 360° is not part of the measurement sector.

d) Cup anemometers free of icing
To eliminate the influence of icing on the wind speed measurements, the MEASNET icing criterion is used. All data acquired by cup anemometers is disregarded if the air temperature, measured at 96 m is lower than 2 °C while the relative humidity is higher than 80 %. The time series of the recorded air temperature is shown in fig. 23.

e) LiDAR availability
All data with LiDAR availability less than 90 % are filtered from the data set. The availability is derived as the ratio of the amount of packets registered in a 10-minute interval and the observed highest common amount (37). Uncommon cases with more than 37 packets are removed.

f) Precipitation
As prescribed by IEC 61400-12-1, no filtering is performed on precipitation.

4 LiDAR Validation KPIs

For each comparison height, the 10-minute averaged wind speed and wind direction measured by the LiDAR are compared to the values obtained with the sensors on the Meteorological Mast 4. We will refer to the LiDAR results as 'rsd' (remote sensing device) and the Meteorological Mast 4 results as 'ref' (reference).

Regression parameters of the wind speed and direction comparisons are identified as Key Performance Indicators (KPIs), which should lie in specified ranges. This is referred to as LiDAR validation and results are presented in this chapter.

4.1 Wind speed comparison

The wind speed plots in figs. 11 to 15 show the raw data, which are the 10-minute averaged wind speed samples, in blue. The deviation, in red, is the relative difference between the wind speeds measured by the ref, v_{ref}, and the rsd, v_{rsd}. The deviation is defined as

$$\text{deviation} = \frac{v_{\text{rsd}} - v_{\text{ref}}}{v_{\text{ref}}} \cdot 100\,\% \tag{4.1}$$

From the raw data, bin-wise mean values are computed, which are represented by square markers. The bin-width equals 0.5 m/s, centred at integer multiples of 0.5 m/s. The first and last bin are only 0.25 m/s wide to fill the 4 m/s to 16 m/s range. The bin-wise mean values of bins that do not meet the bin-count threshold of three samples are omitted.

Two regression methods are applied to the data. The two-parameter (2p) method, a linear regression using a slope and offset, is applied to both the raw data and the bin-wise means (binmeans).
$y_{2p} = \text{slope} \cdot x + \text{offset}$
The one-parameter (1p) method, a linear regression using only a slope that passes through the origin, is applied to the bin-wise means only.
$y_{1p} = \text{slope} \cdot x$

The regression results are shown in the wind speed plots. In these figures the $y_{bin,1p}$ results, which are used as a validation KPI, agree well with the IEC prescribed $y_{bin,2p}$ results, which will be discussed in chapter 5.

4.2 Wind direction comparison

Performing a regression on the wind direction comparison which features a slope - as was done for the wind speed - makes little physical sense, because the value obtained at 0° should match the one at 360°. Therefore, we only consider the offset. This is best visualised by plotting the difference.

The wind direction comparison plots in figs. 6 to 10 show the difference between the wind direction measured by the ref, wd_{ref}, and the rsd, wd_{rsd}. The difference is defined as

$$\Delta_{wd} = wd_{\text{rsd}} - wd_{\text{ref}} \tag{4.2}$$

From the raw data, bin-wise mean values are computed, which are represented by square markers. The bin-width equals 10°. The bin-wise mean values of bins that do not meet the bin-count threshold of three samples are omitted. The regression of the binmeans is in this case simply the mean of the binmeans.

Strong outliers can be caused by the heterodyne detection, which causes the LiDAR to sometimes report the wind direction with a 180° error. The percentage of the samples affected are reported as $\Delta_{90_{\text{WD}}} \equiv |\Delta_{wd}| > 90°$. These outliers strongly influence the binmeans (and standard deviation). To provide an estimate of the offset in the unaffected samples, the median value of Δ_{wd} is shown too.

ECN part of TNO has defined KPIs on wind speed and wind direction regression parameters in the same fashion as the NORSEWinD criteria [3] and the KPIs defined in the 'Carbon Trust Offshore Wind Accelerator roadmap for the commercial acceptance of floating LIDAR technology' [4]. The KPIs are shown in table 1. All criteria are met.

Table 1: LiDAR validation Key Performance Indicators results

KPI	height	result	unit	lower limit	upper limit	status
	m	unit		unit	unit	
$\text{slope}_{\text{WS},1p}$	100	0.985	-	0.98	1.02	pass
	90	0.997	-			pass
	59	0.991	-			pass
	44	0.997	-			pass
	29	0.994	-			pass
$R^2_{\text{WS},1p}$	100	1.000	-	0.98		pass
	90	1.000	-			pass
	59	1.000	-			pass
	44	1.000	-			pass
	29	1.000	-			pass
$\text{offset}_{\text{WD,median}}$	100	-1.987	°	-5	5	pass
	90	-1.840	°			pass
	59	-2.612	°			pass
	44	-1.280	°			pass
	29	-3.475	°			pass
$\Delta_{90_{\text{WD}}}$	100	2.653	%		3	pass
	90	2.678	%			pass
	59	2.421	%			pass
	44	1.556	%			pass
	29	0.000	%			pass

4.3 Availability

This section presents the LiDAR availability KPIs. We use the KPIs as defined in Offshore Wind Accelerator (OWA) roadmap [4].

The monthly availabilities are reported in table 2 per calendar month. Therefore the first and last month contain the data for a fraction of the month. The monthly system availability (MSA) represents the time that the LiDAR system was recording data. The monthly post-processed data availability (MPDA) represents the time that the LiDAR delivered data that passed our filtering criteria. It should be noted that the MPDA is strongly affected by the lower limit that is chosen for the LiDAR availability metric, which we set to 90 %.

Table 2 also lists the overall system availability and the overall data availability for the whole campaign. Only these overall values are evaluated as a KPI. We require the overall system availability to exceed 90 % and the overall data availability to exceed

85 % at each comparison height. The data availability meets these requirements at all comparison heights.

Table 2: LiDAR availability KPIs

month	samples	MSA	MPDA				
			100 m	90 m	59 m	44 m	29 m
		%	%	%	%	%	%
August	144	100.0	99.3	99.3	99.3	99.3	99.3
September	4320	99.9	97.1	97.1	97.1	97.2	97.1
October	1296	100.0	95.6	95.3	95.3	95.2	95.2
overall	**5760**	**99.9**	**96.8**	**96.7**	**96.7**	**96.8**	**96.7**

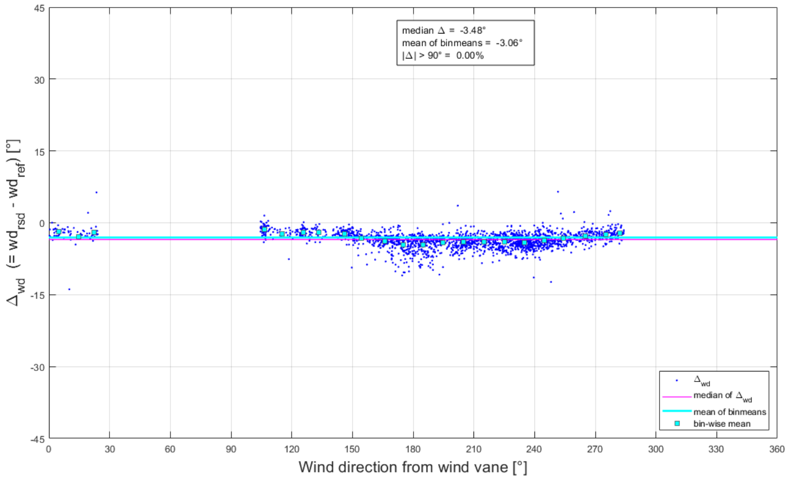

Figure 6: Comparison of 10-minute averages of the wind direction @29 m

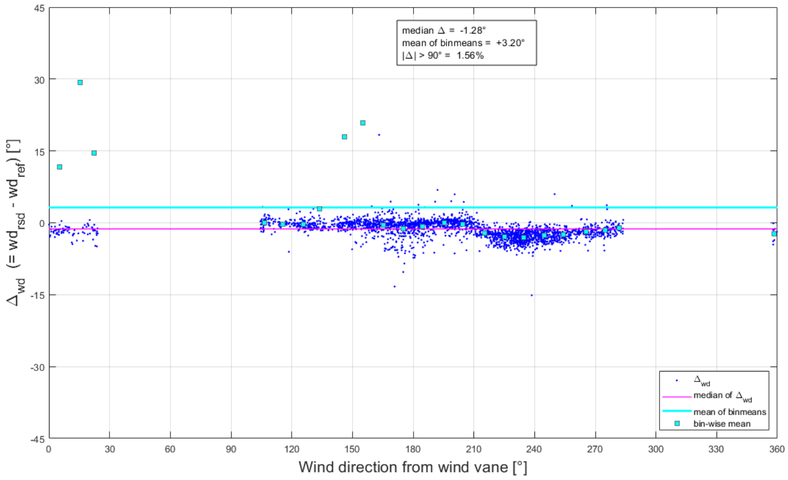

Figure 7: Comparison of 10-minute averages of the wind direction @44 m

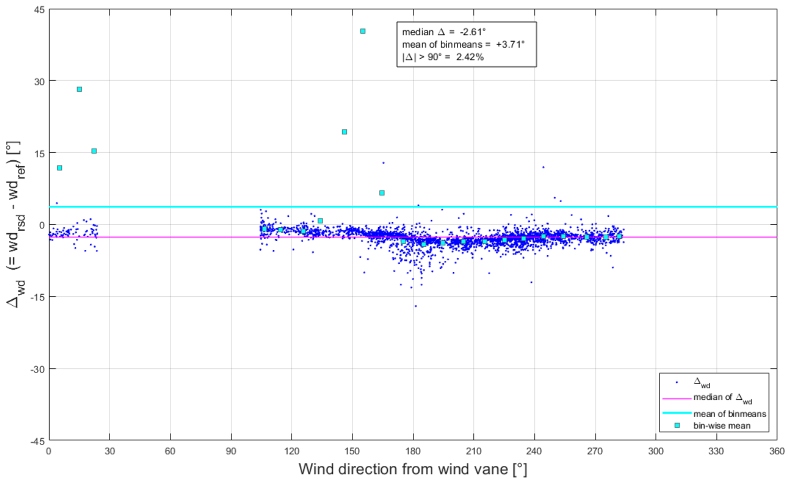

Figure 8: Comparison of 10-minute averages of the wind direction @59 m

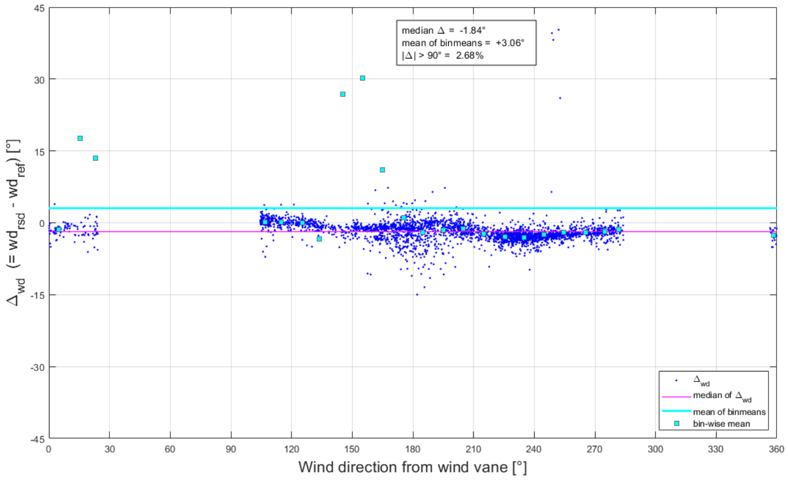

Figure 9: Comparison of 10-minute averages of the wind direction @90 m

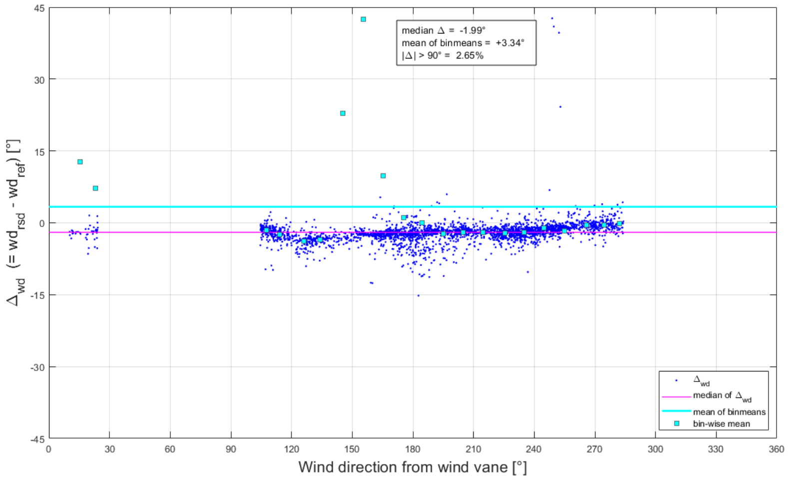

Figure 10: Comparison of 10-minute averages of the wind direction @100 m

5 LiDAR Verification

This chapter reports the results of the LiDAR verification analysis as defined in annex L.3 [5]. The analysis is performed using the in-house software tool *RSDverification* version 1.1.1.

5.1 Direct data comparison

A comparison of the horizontal wind speed between the Meteorological Mast 4 devices and the LiDAR for each comparison height is presented in figs. 11 to 15. The format is taken from figure L.5 [5]. Only samples for which the reference wind speed is in the range of 4 m/s to 16 m/s are used.

5.2 Bin-wise data comparison

The bin-wise comparison described in Annex L.3 [5] first requires binning of the reference wind speeds measured on the Meteorological Mast 4. The prescribed bin width is 0.5 m/s centred on integer multiples of 0.5 m/s. Because the range is 4 m/s to 16 m/s, the first and last bin are given half the prescribed width and are centred at 4.125 m/s and 15.875 m/s respectively.

The resulting bin count histograms are presented in fig. 26. Due to the smaller bin width, the first and last bin have a significantly lower bin count.

All comparison heights have bins in the upper end of the 4 m/s to 16 m/s range that contain less than the minimum of three data sets, specified by data coverage requirement c) [5, L.2.2]. This is a deviation from the standard, reported in chapter 8.

The resulting bin-wise comparisons for each measurement height, are presented in figs. 16 to 20. The results of the regressions are summarised in table 3. The uncertainty intervals shown in these figures are discussed in section 7.1.

Table 3: LiDAR verification IEC 61400-12-1 Annex L results

height	slope	offset	R^2
m	-	m/s	-
100	0.985	-0.003	1.000
90	1.002	-0.056	1.000
59	0.990	0.011	1.000
44	1.007	-0.100	1.000
29	0.983	0.096	1.000

5.3 Systematic uncertainties

The results of the systematic uncertainty analysis, as described in section 7.2, are presented for each comparison height in tables 4 to 8. The tables are modelled after table L.9 [5]. The total LiDAR uncertainty is reported in column 'V_{rsd}'.

If there are fewer than three data sets in any bin, all statistics (mean and standard deviation) and derived properties are omitted from the table.

5.4 Environmental conditions

The uncertainty computation for the LiDAR as part of a future power performance campaign requires the environmental conditions experienced during the LiDAR verification test [5, annex L.7.1, item i]. For completeness we report the environmental conditions even though this verification test is not linked to a power performance campaign. The conditions at each comparison height are reported in tables 9 to 13. The environmental data is subject to the same filtering steps as the (wind speed) data used for the verification analysis. The environmental data is binned against the reference wind speed[1].

In addition to the tabulated sensitivity results, these environmental variables for which a significant sensitivity is found in 14 are also plotted as a function of wind speed along with their distribution in figs. 21 to 22.

[1] For the reference wind speed the bin centre is reported, because each environmental condition may have a slightly difference bin-wise mean wind speed depending on the availability of environmental data.

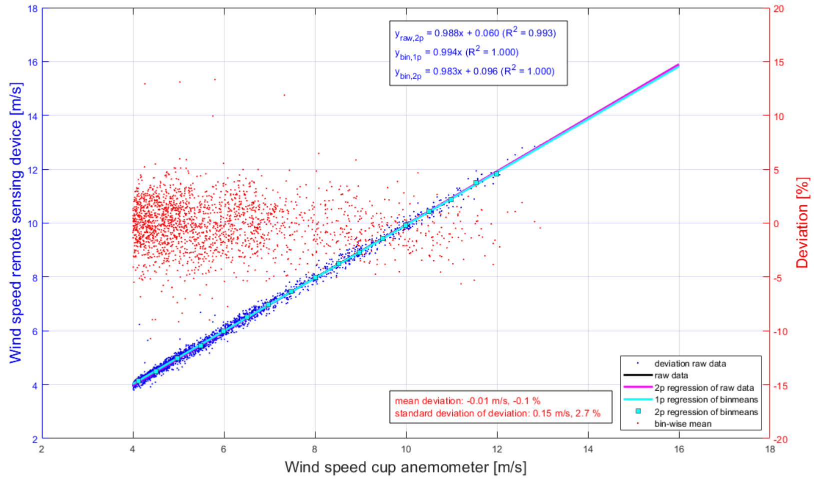

Figure 11: Wind speed comparison @29 m

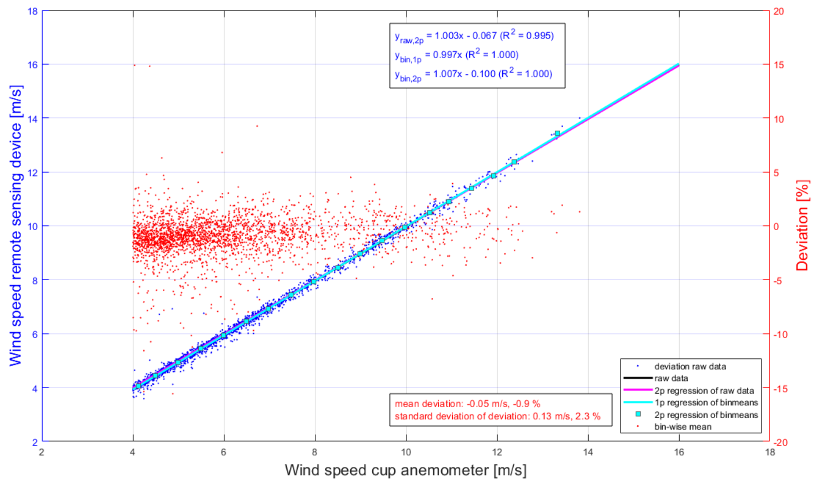

Figure 12: Wind speed comparison @44 m

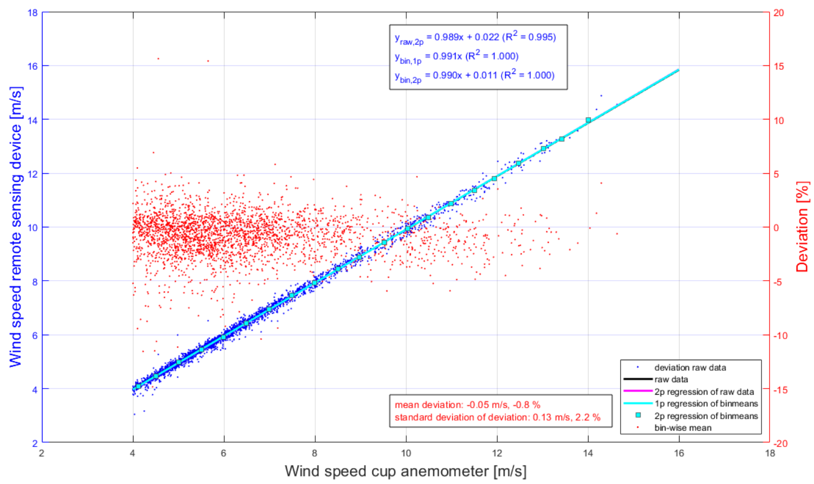

Figure 13: Wind speed comparison @59 m

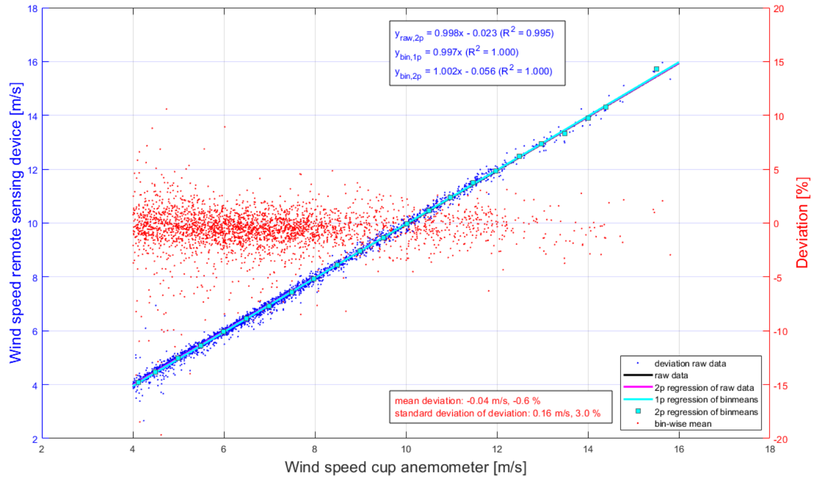

Figure 14: Wind speed comparison @90 m

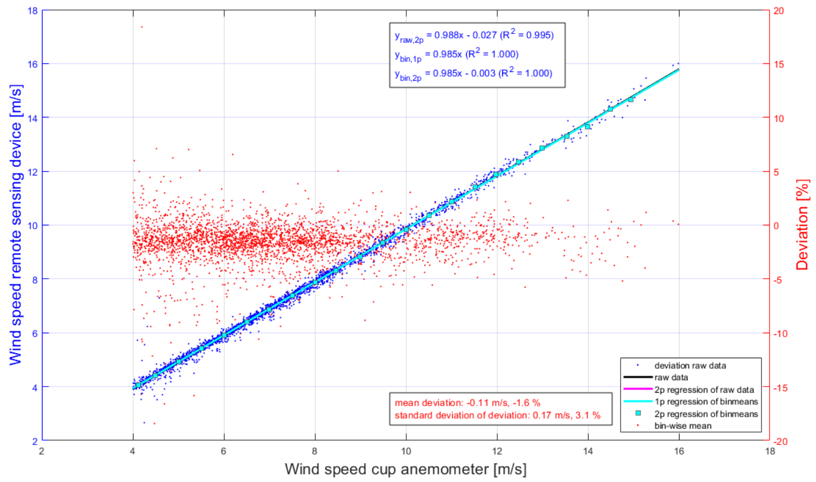

Figure 15: Wind speed comparison @100 m

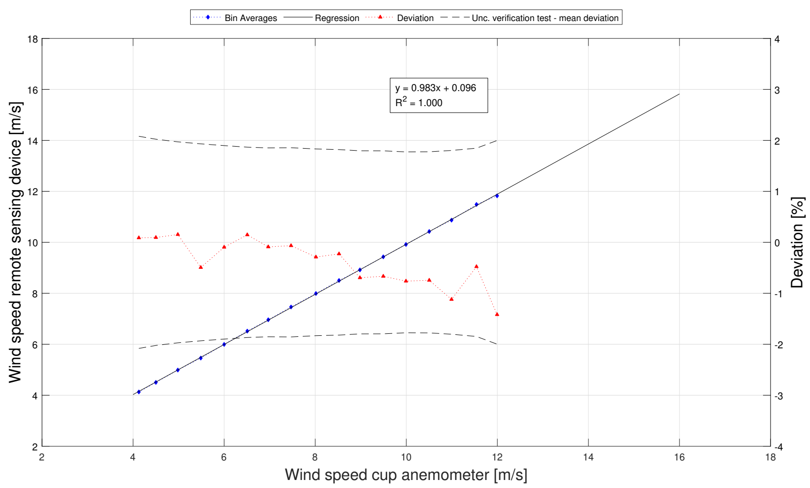

Figure 16: Bin-wise wind speed comparison @29 m

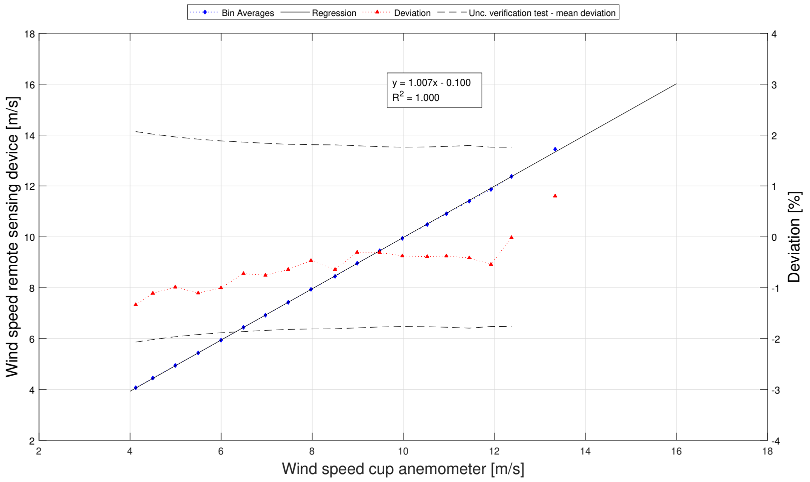

Figure 17: Bin-wise wind speed comparison @44 m

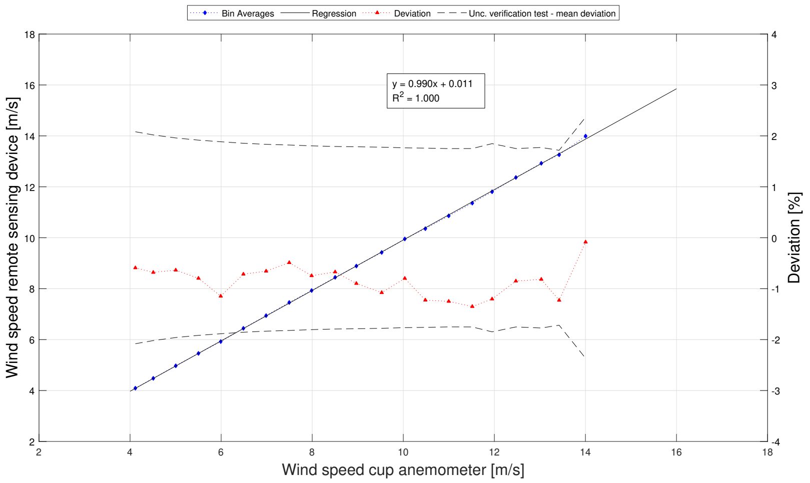

Figure 18: Bin-wise wind speed comparison @59 m

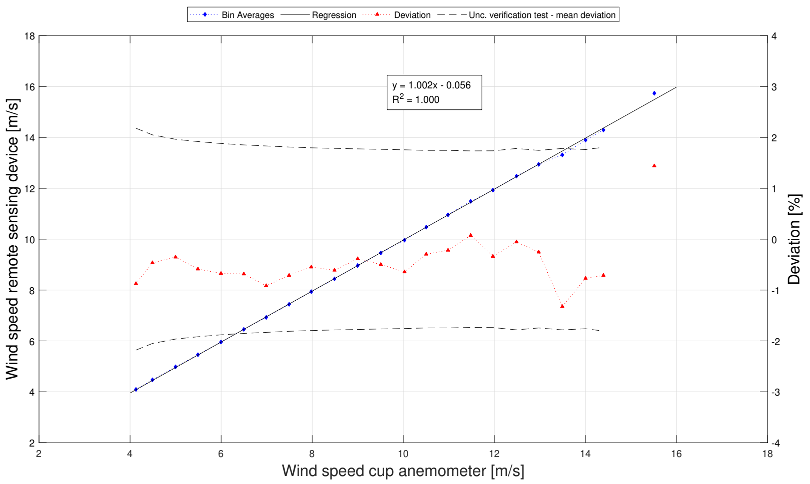

Figure 19: Bin-wise wind speed comparison @90 m

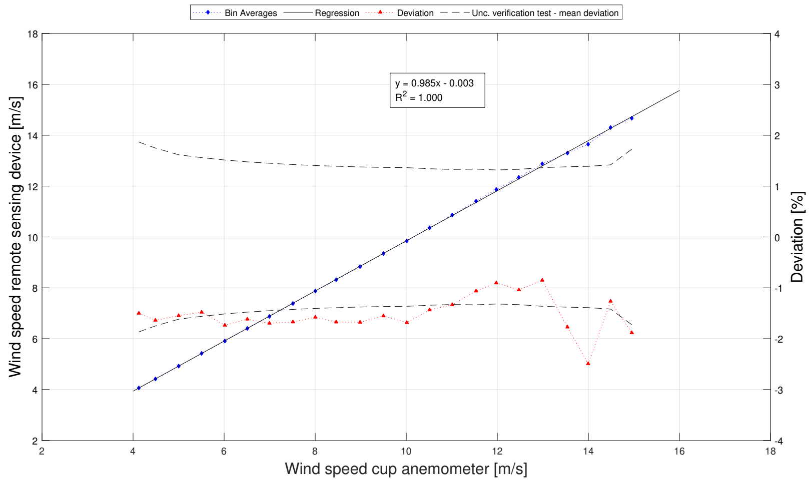

Figure 20: Bin-wise wind speed comparison @100 m

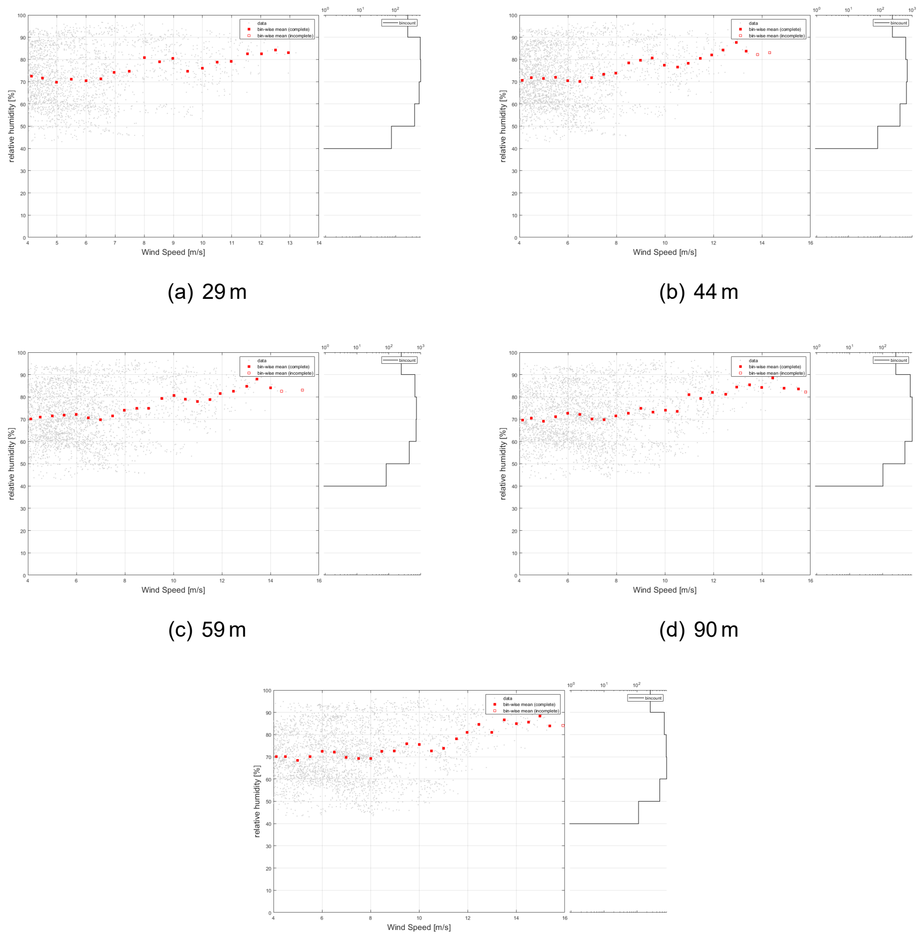

(a) 29 m

(b) 44 m

(c) 59 m

(d) 90 m

(e) 100 m

Figure 21: Environmental conditions: relative humidity

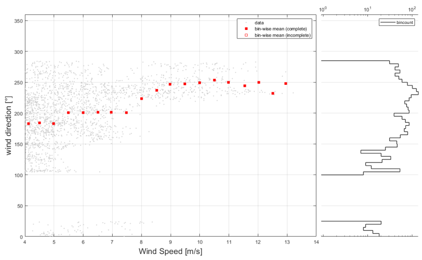

(a) 29 m

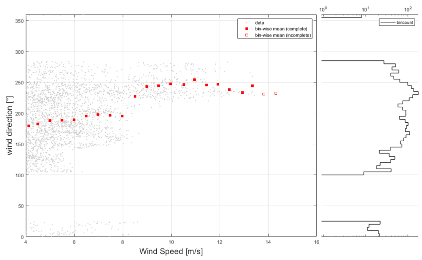

(b) 44 m

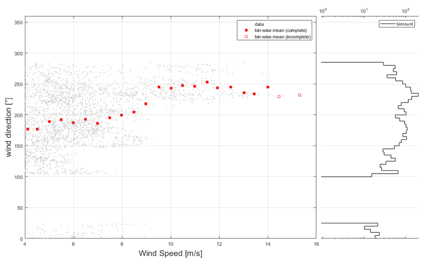

(c) 59 m

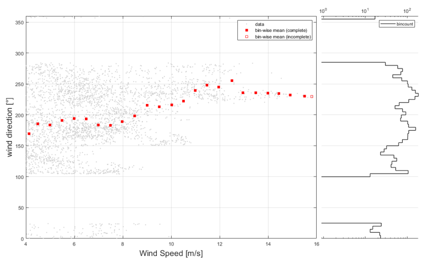

(d) 90 m

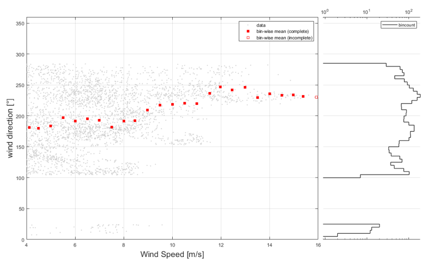

(e) 100 m

Figure 22: Environmental conditions: reference wind direction

Table 4: Uncertainty calculations arising from performance verification of the rsd @29 m in terms of systematic uncertainties.

V_{cup}	V_{rsd}	data sets	V_{rsd} max	V_{rsd} min	V_{rsd} std	$V_{\mathrm{rsd}} \frac{\mathrm{std}}{\sqrt{n}}$	mean deviation	V_{cup} uncertainty	mounting unc. rsd	separation unc.	V_{rsd} uncertainty
m/s	**m/s**	**#**	**m/s**	**m/s**	**m/s**	**m/s**	**%**	**%**	**%**	**%**	**%**
4.13	4.13	242	6.24	3.80	0.176	0.011	0.089	2.033	0.10	0.18	2.083
4.50	4.50	387	5.64	3.92	0.191	0.010	0.095	1.981	0.10	0.18	2.025
4.98	4.99	309	5.69	4.52	0.191	0.011	0.153	1.928	0.10	0.18	1.977
5.49	5.46	216	6.69	5.06	0.198	0.013	-0.493	1.884	0.10	0.18	1.994
6.00	5.99	186	6.58	5.56	0.204	0.015	-0.096	1.849	0.10	0.18	1.900
6.51	6.52	179	6.92	5.96	0.193	0.014	0.147	1.820	0.10	0.18	1.872
6.97	6.96	105	7.40	6.56	0.194	0.019	-0.089	1.799	0.10	0.18	1.854
7.47	7.46	64	8.20	7.01	0.236	0.030	-0.065	1.779	0.10	0.18	1.857
8.02	7.99	59	8.61	7.50	0.222	0.029	-0.289	1.761	0.10	0.18	1.854
8.52	8.50	59	9.00	7.97	0.242	0.031	-0.227	1.747	0.10	0.18	1.833
8.98	8.92	63	9.43	8.47	0.214	0.027	-0.694	1.736	0.10	0.18	1.925
9.49	9.43	41	9.91	8.89	0.214	0.033	-0.666	1.725	0.10	0.18	1.914
9.99	9.92	48	10.43	9.41	0.198	0.029	-0.761	1.716	0.10	0.18	1.930
10.50	10.43	34	10.97	9.99	0.212	0.036	-0.744	1.707	0.10	0.18	1.926
10.99	10.87	27	11.29	10.27	0.278	0.054	-1.119	1.700	0.10	0.18	2.121
11.54	11.49	16	11.94	10.89	0.301	0.075	-0.477	1.693	0.10	0.18	1.907
11.99	11.82	6	12.36	11.46	0.297	0.121	-1.418	1.687	0.10	0.18	2.450
		2	12.79	12.53							
		2	12.89	12.85							
		0									
		0									
		0									
		0									
		0									
		0									

Table 5: Uncertainty calculations arising from performance verification of the rsd @44 m in terms of systematic uncertainties.

V_{cup}	V_{rsd}	data sets	V_{rsd} max	V_{rsd} min	V_{rsd} std	$V_{\text{rsd}} \frac{\text{std}}{\sqrt{n}}$	mean deviation	V_{cup} uncertainty	mounting unc. rsd	separation unc.	V_{rsd} uncertainty
m/s	m/s	#	m/s	m/s	m/s	m/s	%	%	%	%	%
4.12	4.07	200	4.64	3.59	0.119	0.008	-1.334	2.033	0.10	0.12	2.461
4.50	4.45	445	6.72	3.92	0.202	0.010	-1.109	1.981	0.10	0.12	2.303
4.99	4.94	399	6.92	4.12	0.197	0.010	-0.989	1.927	0.10	0.12	2.198
5.50	5.43	338	6.76	4.71	0.190	0.010	-1.104	1.883	0.10	0.12	2.215
6.00	5.94	272	6.37	5.40	0.180	0.011	-1.004	1.849	0.10	0.12	2.136
6.49	6.44	198	7.35	5.77	0.195	0.014	-0.722	1.821	0.10	0.12	1.997
6.97	6.92	146	7.28	6.32	0.174	0.014	-0.755	1.799	0.10	0.12	1.988
7.47	7.42	132	7.89	6.97	0.171	0.015	-0.642	1.779	0.10	0.12	1.929
7.97	7.94	81	8.50	7.58	0.190	0.021	-0.467	1.763	0.10	0.12	1.870
8.50	8.45	51	8.82	7.98	0.200	0.028	-0.642	1.748	0.10	0.12	1.918
8.99	8.96	55	9.40	8.48	0.198	0.027	-0.304	1.736	0.10	0.12	1.816
9.48	9.45	74	9.86	8.94	0.198	0.023	-0.307	1.725	0.10	0.12	1.798
9.98	9.94	48	10.38	9.57	0.167	0.024	-0.376	1.716	0.10	0.12	1.802
10.53	10.48	45	10.92	9.86	0.227	0.034	-0.389	1.707	0.10	0.12	1.808
10.95	10.90	31	11.46	10.41	0.246	0.044	-0.377	1.701	0.10	0.12	1.816
11.45	11.40	21	11.82	10.91	0.262	0.057	-0.414	1.694	0.10	0.12	1.842
11.93	11.86	18	12.31	11.41	0.197	0.046	-0.543	1.688	0.10	0.12	1.843
12.38	12.37	11	12.64	12.11	0.165	0.050	-0.016	1.683	0.10	0.12	1.760
		2	13.38	12.40							
13.34	13.44	3	13.69	13.23	0.233	0.135	0.800	1.674	0.10	0.12	2.137
		1	14.00	14.00							
		0									
		0									
		0									
		0									

Table 6: Uncertainty calculations arising from performance verification of the rsd @59 m in terms of systematic uncertainties.

V_{cup}	V_{rsd}	data sets	V_{rsd} max	V_{rsd} min	V_{rsd} std	V_{rsd} $\frac{std}{\sqrt{n}}$	mean deviation	V_{cup} uncertainty	mounting unc. rsd	separation unc.	V_{rsd} uncertainty
m/s	m/s	#	m/s	m/s	m/s	m/s	%	%	%	%	%
4.12	4.09	139	4.40	3.05	0.150	0.013	-0.591	2.035	0.10	0.09	2.163
4.51	4.48	324	5.27	3.17	0.200	0.011	-0.681	1.980	0.10	0.09	2.131
5.00	4.97	386	5.99	4.43	0.183	0.009	-0.635	1.926	0.10	0.09	2.060
5.50	5.46	352	6.52	4.98	0.185	0.010	-0.796	1.883	0.10	0.09	2.076
5.99	5.92	302	6.39	5.43	0.200	0.011	-1.148	1.849	0.10	0.09	2.207
6.49	6.44	279	6.84	5.84	0.179	0.011	-0.715	1.821	0.10	0.09	1.988
6.99	6.94	226	7.54	6.11	0.195	0.013	-0.656	1.798	0.10	0.09	1.948
7.50	7.46	138	7.90	6.79	0.208	0.018	-0.489	1.778	0.10	0.09	1.885
7.99	7.93	117	8.33	7.52	0.201	0.019	-0.746	1.762	0.10	0.09	1.953
8.50	8.45	90	9.03	7.93	0.198	0.021	-0.671	1.748	0.10	0.09	1.914
8.97	8.89	60	9.28	8.49	0.198	0.026	-0.898	1.736	0.10	0.09	2.000
9.53	9.42	55	9.87	9.01	0.215	0.029	-1.077	1.724	0.10	0.09	2.079
10.03	9.95	65	10.72	9.46	0.226	0.028	-0.798	1.715	0.10	0.09	1.937
10.48	10.36	56	10.92	9.90	0.230	0.031	-1.225	1.707	0.10	0.09	2.144
11.00	10.86	44	11.36	10.32	0.205	0.031	-1.249	1.700	0.10	0.09	2.151
11.52	11.36	38	12.00	10.97	0.231	0.037	-1.351	1.693	0.10	0.09	2.212
11.95	11.81	16	12.44	11.43	0.328	0.082	-1.203	1.688	0.10	0.09	2.205
12.47	12.37	18	12.75	12.01	0.199	0.047	-0.850	1.682	0.10	0.09	1.947
13.03	12.92	13	13.20	12.45	0.227	0.063	-0.817	1.677	0.10	0.09	1.952
13.42	13.26	3	13.32	13.21	0.054	0.031	-1.228	1.673	0.10	0.09	2.111
14.00	13.99	3	14.37	13.57	0.400	0.231	-0.085	1.668	0.10	0.09	2.368
		2	14.88	14.55							
		0									
		0									
		0									

Table 7: Uncertainty calculations arising from performance verification of the rsd @90 m in terms of systematic uncertainties.

V_{cup}	V_{rsd}	data sets	V_{rsd} max	V_{rsd} min	V_{rsd} std	$V_{\text{rsd}}\,\frac{\text{std}}{\sqrt{n}}$	mean deviation	V_{cup} uncertainty	mounting unc. rsd	separation unc.	V_{rsd} uncertainty
m/s	**m/s**	**#**	**m/s**	**m/s**	**m/s**	**m/s**	**%**	**%**	**%**	**%**	**%**
4.13	4.09	123	5.10	1.65	0.334	0.030	-0.875	2.033	0.10	0.06	2.349
4.49	4.47	271	6.94	1.71	0.315	0.019	-0.465	1.982	0.10	0.06	2.102
5.00	4.98	254	5.51	4.29	0.183	0.011	-0.353	1.926	0.10	0.06	1.995
5.49	5.46	278	5.95	4.52	0.180	0.011	-0.587	1.884	0.10	0.06	2.006
6.00	5.96	312	6.56	5.45	0.167	0.009	-0.674	1.849	0.10	0.06	1.997
6.50	6.45	295	6.83	5.78	0.174	0.010	-0.684	1.821	0.10	0.06	1.975
6.99	6.92	260	7.42	6.22	0.199	0.012	-0.915	1.798	0.10	0.06	2.048
7.49	7.44	270	8.04	6.77	0.192	0.012	-0.712	1.779	0.10	0.06	1.946
7.98	7.94	186	8.33	7.43	0.175	0.013	-0.548	1.762	0.10	0.06	1.877
8.49	8.44	123	8.97	7.97	0.181	0.016	-0.610	1.748	0.10	0.06	1.886
9.00	8.96	97	9.45	8.64	0.192	0.019	-0.386	1.736	0.10	0.06	1.817
9.51	9.46	88	9.91	8.96	0.198	0.021	-0.498	1.725	0.10	0.06	1.834
10.03	9.96	77	10.33	9.49	0.201	0.023	-0.644	1.715	0.10	0.06	1.871
10.50	10.47	83	10.97	10.04	0.188	0.021	-0.296	1.707	0.10	0.06	1.770
10.98	10.96	51	11.36	10.47	0.197	0.028	-0.218	1.700	0.10	0.06	1.759
11.48	11.49	63	11.99	11.05	0.206	0.026	0.073	1.693	0.10	0.06	1.737
11.97	11.93	53	12.60	11.08	0.242	0.033	-0.338	1.688	0.10	0.06	1.770
12.49	12.48	12	12.87	12.19	0.219	0.063	-0.055	1.682	0.10	0.06	1.783
12.97	12.94	17	13.38	12.65	0.201	0.049	-0.254	1.677	0.10	0.06	1.764
13.49	13.31	12	13.74	12.99	0.251	0.073	-1.325	1.673	0.10	0.06	2.221
14.00	13.90	11	14.24	13.60	0.220	0.066	-0.769	1.668	0.10	0.06	1.921
14.40	14.29	8	14.74	13.87	0.256	0.091	-0.712	1.665	0.10	0.06	1.941
		2	15.11	14.50							
15.51	15.74	3	15.96	15.61	0.197	0.114	1.439	1.658	0.10	0.06	2.334
		1	15.34	15.34							

Table 8: Uncertainty calculations arising from performance verification of the rsd @100 m in terms of systematic uncertainties.

V_{cup}	V_{rsd}	data sets	V_{rsd} max	V_{rsd} min	V_{rsd} std	$V_{\text{rsd}} \frac{\text{std}}{\sqrt{n}}$	mean deviation	V_{cup} uncertainty	mounting unc. rsd	separation unc.	V_{rsd} uncertainty
m/s	**m/s**	**#**	**m/s**	**m/s**	**m/s**	**m/s**	**%**	**%**	**%**	**%**	**%**
4.13	4.06	114	5.73	1.69	0.313	0.029	-1.499	1.698	0.10	0.05	2.393
4.49	4.42	241	7.29	1.60	0.372	0.024	-1.637	1.637	0.10	0.05	2.395
5.00	4.92	260	5.59	4.18	0.198	0.012	-1.546	1.568	0.10	0.05	2.236
5.51	5.42	249	5.85	4.50	0.187	0.012	-1.478	1.515	0.10	0.05	2.149
6.02	5.91	274	6.60	5.29	0.180	0.011	-1.734	1.471	0.10	0.05	2.301
6.51	6.40	292	6.81	5.72	0.175	0.010	-1.616	1.436	0.10	0.05	2.189
6.99	6.88	259	7.30	6.05	0.183	0.011	-1.695	1.408	0.10	0.05	2.230
7.51	7.39	258	7.92	6.92	0.188	0.012	-1.670	1.382	0.10	0.05	2.194
8.00	7.88	214	8.32	7.41	0.192	0.013	-1.577	1.362	0.10	0.05	2.111
8.46	8.32	158	8.94	7.76	0.193	0.015	-1.672	1.345	0.10	0.05	2.174
8.98	8.83	105	9.26	8.30	0.188	0.018	-1.675	1.328	0.10	0.05	2.169
9.50	9.35	98	9.76	8.62	0.213	0.021	-1.551	1.313	0.10	0.05	2.067
10.01	9.84	71	10.40	9.33	0.228	0.027	-1.682	1.301	0.10	0.05	2.165
10.51	10.36	80	10.87	9.95	0.198	0.022	-1.434	1.290	0.10	0.05	1.963
11.01	10.86	95	11.34	10.47	0.193	0.020	-1.331	1.280	0.10	0.05	1.880
11.53	11.41	53	11.87	10.99	0.224	0.031	-1.062	1.271	0.10	0.05	1.705
11.98	11.87	60	12.45	11.39	0.201	0.026	-0.903	1.264	0.10	0.05	1.597
12.47	12.34	36	12.99	11.83	0.234	0.039	-1.039	1.257	0.10	0.05	1.688
12.99	12.88	13	13.19	12.53	0.210	0.058	-0.850	1.250	0.10	0.05	1.606
13.54	13.30	14	13.87	12.85	0.262	0.070	-1.771	1.243	0.10	0.05	2.245
13.99	13.65	12	14.03	13.24	0.266	0.077	-2.490	1.238	0.10	0.05	2.851
14.49	14.30	12	14.67	13.80	0.317	0.091	-1.263	1.233	0.10	0.05	1.899
14.95	14.67	6	15.17	13.99	0.429	0.175	-1.882	1.229	0.10	0.05	2.553
		2	15.46	14.65							
		2	16.00	15.93							

Table 9: Environmental conditions experienced during verification test for LiDAR measurements @29 m.

wind speed	shear exponent	turbulence intensity	precipitation	wind direction	air temperature	relative humidity	air density	flow inclination	wind veer
m/s	**-**	**%**	**%**	**°**	**°C**	**%**	**kg/m³**	**°**	**°/m**
4.125	0.2455	8.83	2.52	179.4	18.06	70.58	1.198	2.679	-0.1386
4.500	0.2902	8.17	1.70	182.4	17.42	71.73	1.202	2.485	-0.1257
5.000	0.2770	9.06	2.83	187.8	17.52	71.40	1.200	2.381	-0.1229
5.500	0.2793	9.52	3.04	188.7	17.53	71.96	1.199	1.961	-0.0897
6.000	0.2871	9.97	4.38	188.9	17.75	70.47	1.198	1.992	-0.0861
6.500	0.2485	11.31	6.78	195.2	17.62	70.03	1.198	1.896	-0.0646
7.000	0.2218	11.92	8.32	197.6	17.43	71.72	1.198	1.811	-0.0490
7.500	0.2526	11.27	12.80	196.7	16.80	73.32	1.199	1.639	-0.0428
8.000	0.2247	11.85	12.49	195.1	17.01	73.83	1.200	1.409	-0.0268
8.500	0.1929	12.36	9.22	227.3	17.02	78.39	1.200	1.347	-0.0005
9.000	0.2039	12.80	7.36	243.1	17.05	79.58	1.198	1.261	0.0068
9.500	0.1912	12.57	6.83	244.5	17.03	80.62	1.199	1.269	0.0121
10.000	0.1615	12.66	13.16	247.2	17.05	77.50	1.199	0.978	0.0137
10.500	0.1446	12.07	4.82	246.3	17.44	76.64	1.199	0.923	0.0177
11.000	0.1367	12.19	13.96	253.9	17.12	78.26	1.197	0.774	0.0176
11.500	0.1580	13.33	10.00	245.6	17.21	80.47	1.197	0.835	0.0130
12.000	0.1543	13.08	17.07	246.7	17.30	81.98	1.194	0.781	0.0219
12.500	0.1861	13.31	10.13	238.4	17.43	84.24	1.194	0.824	0.0212
13.000	0.1824	13.11	71.43	233.1	17.38	87.57	1.192	0.266	0.0153
13.500	0.1580	13.77	44.00	244.5	17.18	83.74	1.193	0.500	0.0206
14.000									
14.500									
15.000									
15.500									
15.875									

Table 10: Environmental conditions experienced during verification test for LiDAR measurements @44 m.

wind speed	shear exponent	turbulence intensity	precipitation	wind direction	air temperature	relative humidity	air density	flow inclination	wind veer
m/s	-	%	%	°	°C	%	kg/m³	°	°/m
4.125	0.2455	8.83	2.52	179.4	18.06	70.58	1.198	2.679	-0.1386
4.500	0.2902	8.17	1.70	182.4	17.42	71.73	1.202	2.485	-0.1257
5.000	0.2770	9.06	2.83	187.8	17.52	71.40	1.200	2.381	-0.1229
5.500	0.2793	9.52	3.04	188.7	17.53	71.96	1.199	1.961	-0.0897
6.000	0.2871	9.97	4.38	188.9	17.75	70.47	1.198	1.992	-0.0861
6.500	0.2485	11.31	6.78	195.2	17.62	70.03	1.198	1.896	-0.0646
7.000	0.2218	11.92	8.32	197.6	17.43	71.72	1.198	1.811	-0.0490
7.500	0.2526	11.27	12.80	196.7	16.80	73.32	1.199	1.639	-0.0428
8.000	0.2247	11.85	12.49	195.1	17.01	73.83	1.200	1.409	-0.0268
8.500	0.1929	12.36	9.22	227.3	17.02	78.39	1.200	1.347	-0.0005
9.000	0.2039	12.80	7.36	243.1	17.05	79.58	1.198	1.261	0.0068
9.500	0.1912	12.57	6.83	244.5	17.03	80.62	1.199	1.269	0.0121
10.000	0.1615	12.66	13.16	247.2	17.05	77.50	1.199	0.978	0.0137
10.500	0.1446	12.07	4.82	246.3	17.44	76.64	1.199	0.923	0.0177
11.000	0.1367	12.19	13.96	253.9	17.12	78.26	1.197	0.774	0.0176
11.500	0.1580	13.33	10.00	245.6	17.21	80.47	1.197	0.835	0.0130
12.000	0.1543	13.08	17.07	246.7	17.30	81.98	1.194	0.781	0.0219
12.500	0.1861	13.31	10.13	238.4	17.43	84.24	1.194	0.824	0.0212
13.000	0.1824	13.11	71.43	233.1	17.38	87.57	1.192	0.266	0.0153
13.500	0.1580	13.77	44.00	244.5	17.18	83.74	1.193	0.500	0.0206
14.000									
14.500									
15.000									
15.500									
15.875									

Table 11: Environmental conditions experienced during verification test for LiDAR measurements @59 m.

wind speed	shear exponent	turbulence intensity	precipitation	wind direction	air temperature	relative humidity	air density	flow inclination	wind veer
m/s	**-**	**%**	**%**	**°**	**°C**	**%**	**kg/m³**	**°**	**°/m**
4.125	0.1912	8.81	1.48	176.8	18.25	70.16	1.198	2.836	-0.1345
4.500	0.2362	8.80	2.40	177.2	17.89	70.95	1.200	2.723	-0.1172
5.000	0.2874	8.69	2.19	189.4	17.57	71.43	1.201	2.518	-0.1275
5.500	0.2969	8.55	2.81	192.6	17.69	71.80	1.199	2.153	-0.1156
6.000	0.2937	9.11	3.39	187.3	17.57	72.15	1.198	1.975	-0.1068
6.500	0.2916	9.56	3.40	193.0	17.71	70.68	1.197	1.877	-0.0841
7.000	0.2841	9.66	4.35	186.3	18.12	69.77	1.196	1.866	-0.0997
7.500	0.2620	10.88	9.74	195.5	17.11	71.53	1.199	1.822	-0.0666
8.000	0.2646	10.91	9.26	199.7	16.68	74.00	1.200	1.602	-0.0522
8.500	0.2962	10.60	19.78	204.7	16.66	74.81	1.200	1.563	-0.0413
9.000	0.2363	11.50	10.54	218.2	16.63	74.80	1.202	1.504	-0.0209
9.500	0.1978	12.81	4.36	245.0	17.09	79.35	1.198	1.257	0.0081
10.000	0.1965	12.80	10.74	243.0	17.01	80.61	1.200	1.206	0.0119
10.500	0.1688	12.31	6.82	247.2	17.16	78.90	1.199	1.098	0.0113
11.000	0.1569	12.57	10.69	246.0	17.36	77.87	1.198	0.846	0.0184
11.500	0.1450	12.42	9.59	253.0	17.17	78.71	1.198	0.860	0.0125
12.000	0.1693	13.75	11.11	243.8	17.08	81.50	1.198	0.830	0.0154
12.500	0.1672	13.27	17.78	244.9	17.34	82.49	1.194	0.758	0.0202
13.000	0.1962	13.58	16.84	236.0	17.41	84.68	1.194	0.913	0.0197
13.500	0.1820	12.98	42.00	234.2	17.26	87.91	1.193	0.480	0.0189
14.000	0.1580	13.12	59.14	245.0	17.11	84.08	1.193	0.449	0.0175
14.500									
15.000									
15.500									
15.875									

Table 12: Environmental conditions experienced during verification test for LiDAR measurements @90 m.

wind speed	shear exponent	turbulence intensity	precipitation	wind direction	air temperature	relative humidity	air density	flow inclination	wind veer
m/s	-	%	%	°	°C	%	kg/m³	°	°/m
4.125	0.1715	8.24	2.29	169.5	18.30	69.51	1.198	2.916	-0.1104
4.500	0.2056	8.07	2.51	185.8	17.89	70.49	1.201	2.825	-0.1200
5.000	0.2116	8.50	1.51	183.4	17.41	69.08	1.203	2.821	-0.0987
5.500	0.2560	7.54	2.43	190.8	17.84	71.11	1.200	2.335	-0.1278
6.000	0.2809	7.27	3.10	194.3	17.64	72.61	1.199	2.113	-0.1237
6.500	0.3086	7.45	3.51	193.7	17.99	72.09	1.196	2.086	-0.1196
7.000	0.2966	7.44	1.98	183.7	18.21	70.14	1.195	1.840	-0.0918
7.500	0.3174	6.91	2.44	182.8	18.49	69.69	1.193	1.825	-0.1128
8.000	0.3102	7.01	6.70	189.1	17.94	71.40	1.196	1.732	-0.1129
8.500	0.3218	7.30	10.19	198.1	16.52	72.58	1.202	1.741	-0.1030
9.000	0.2847	8.55	14.63	215.7	16.53	74.94	1.200	1.619	-0.0501
9.500	0.3127	8.85	11.52	213.1	17.08	73.21	1.198	1.733	-0.0443
10.000	0.2911	8.20	13.54	216.3	16.60	74.10	1.201	1.514	-0.0498
10.500	0.2536	8.85	4.05	222.1	16.82	73.52	1.201	1.516	-0.0260
11.000	0.2044	10.04	11.76	239.6	17.07	80.98	1.200	1.072	0.0065
11.500	0.1707	10.43	7.46	248.3	17.28	79.29	1.199	0.940	0.0128
12.000	0.1921	10.42	8.96	245.0	17.33	82.03	1.198	0.933	0.0104
12.500	0.1710	11.29	18.00	255.2	16.67	81.12	1.199	0.759	0.0180
13.000	0.2072	10.96	12.86	236.0	17.26	84.41	1.197	0.916	0.0095
13.500	0.2091	12.14	9.52	235.5	17.38	85.44	1.194	0.889	0.0157
14.000	0.1913	10.51	13.77	235.4	17.39	84.25	1.195	1.034	0.0160
14.500	0.1990	11.04	43.33	234.3	17.14	88.48	1.194	0.695	0.0202
15.000	0.2059	10.88	33.33	232.4	17.60	83.95	1.193	0.794	0.0248
15.500	0.2056	12.38	31.91	230.2	17.80	83.64	1.191	0.431	0.0230
15.875									

Table 13: Environmental conditions experienced during verification test for LiDAR measurements @100 m.

wind speed	shear exponent	turbulence intensity	precipitation	wind direction	air temperature	relative humidity	air density	flow inclination	wind veer
m/s	-	%	%	°	°C	%	kg/m³	°	°/m
4.125	0.1559	8.76	1.67	181.4	18.94	70.03	1.195	2.997	-0.1146
4.500	0.1908	7.90	2.09	180.2	18.07	70.06	1.200	2.992	-0.1144
5.000	0.2062	8.54	2.13	183.7	17.54	68.44	1.203	2.852	-0.1039
5.500	0.2423	7.88	1.24	197.2	17.91	70.18	1.200	2.441	-0.1122
6.000	0.2621	7.36	4.00	191.7	17.78	72.46	1.198	2.217	-0.1240
6.500	0.2960	7.35	3.40	195.3	18.04	72.23	1.196	2.133	-0.1264
7.000	0.2919	7.42	2.64	192.7	18.58	69.75	1.194	1.934	-0.1072
7.500	0.3129	7.06	0.94	182.1	18.63	69.17	1.193	1.883	-0.1043
8.000	0.3261	6.62	4.25	191.6	18.64	69.24	1.193	1.808	-0.1225
8.500	0.3449	6.68	7.95	192.5	17.55	72.47	1.197	1.791	-0.1239
9.000	0.3111	7.69	11.85	209.4	16.29	72.67	1.203	1.677	-0.0803
9.500	0.2924	8.60	12.25	217.7	16.17	75.93	1.201	1.680	-0.0475
10.000	0.3123	8.56	17.04	218.6	16.95	75.50	1.197	1.660	-0.0417
10.500	0.2845	8.53	9.19	220.4	16.93	72.73	1.200	1.558	-0.0435
11.000	0.2602	8.36	5.67	219.9	16.81	73.89	1.202	1.447	-0.0301
11.500	0.2048	9.68	6.69	236.5	17.33	78.16	1.200	1.111	0.0019
12.000	0.1793	10.46	9.09	247.1	17.30	80.94	1.199	0.928	0.0125
12.500	0.2156	10.27	12.13	242.1	17.19	84.60	1.198	0.995	0.0074
13.000	0.1742	10.71	17.50	246.0	16.96	80.92	1.198	0.724	0.0120
13.500	0.2315	11.04	14.64	229.4	17.29	86.65	1.197	1.064	0.0108
14.000	0.2000	10.91	14.94	235.9	17.40	84.97	1.195	0.874	0.0172
14.500	0.1968	10.90	6.88	233.6	17.35	85.69	1.193	1.011	0.0155
15.000	0.1980	10.72	51.57	233.8	17.10	88.33	1.194	0.652	0.0195
15.500	0.2059	10.76	33.33	231.4	17.60	83.95	1.193	0.794	0.0248
15.875									

6 Sensitivities

This chapter investigates the sensitivity of the LiDAR measurement for various environmental variables (EVs). The sensitivity analysis is performed in accordance with the classification analysis specified in annex L.2 [5]. However, for this analysis we use the same dataset as for the verification analysis. As a result the wind speed range is restricted to 4 m/s to 16 m/s.

6.1 Sensitivity analysis

The basis of this analysis is the deviation between the wind speeds measured by the ref, v_{ref}, and the rsd, v_{rsd}. The deviation is defined in eq. (4.1). Subsequently the sensitivity of this deviation is tested against various EVs. The list of variables is based on table L.2 [5]. The variables considered are described below.

Unless stated otherwise the EVs are height-independent, meaning the same value was used for the sensitivity analysis at each comparison height.

1. **Shear exponent [-]**
   The shear exponent, α, is computed by fitting a power law wind shear model through the v_{ref} measurements at 44 m, 59 m, 90 m and 100 m. The power law is defined by
   $$\frac{v_{\text{ref}}}{v_r} = \left(\frac{h}{h_r}\right)^{\alpha} \tag{6.1}$$

2. **Reference turbulence intensity [-]**
   The reference turbulence intensity, measured by MM4, is defined by
   $$\text{reference turbulence intensity} = \frac{\text{std}(v_{\text{ref}})}{\text{mean}(v_{\text{ref}})} \tag{6.2}$$
   This variable is height-dependent.

3. **Precipitation [%]**
   The rain sensor returns a 0 % to 100 % signal indicating the amount of time precipitation was detected in the 10-minute interval. The precipitation is measured at 96 m.

4. **Reference wind direction [°]**
   The wind direction, as measured by MM4, is height-dependent.

5. **Air temperature [°C]**
   The air temperature is measured at 96 m.

6. **Relative humidity [%RH]**
   The relative humidity is measured at 96 m. (The relative humidity was added to the list of EVs, because it used as in the MEASNET icing criterion in chapter 3.)

7. **Air density [kg/m^3]**
   The air density is computed from the air pressure, air temperature and relative humidity, all measured at 96 m in accordance with equation (12) of IEC 61400-12-1:2017.

8. **Flow inclination [°]**
   The flow inclination is defined as

$$\text{flow inclination} = \arctan\left(\frac{v_{\text{vert}}}{v_{\text{hor}}}\right) \tag{6.3}$$

   The horizontal (v_{hor}) and vertical (v_{vert}) wind speed components are measured by a sonic anemometer at a height of 87 m.

9. **Wind veer [°/m]**
   The wind veer is computed as the difference between the wind direction measurements by MM4 at 42 m and 97 m, divided by the height difference. This definition was taken from IEC 61400-12-1:2017.

$$\text{wind veer} = \frac{v_{d,42} - v_{d,97}}{97 - 42} \tag{6.4}$$

10. **Reference wind speed [m/s]**
    This wind speed, as measured by MM4, is height-dependent.

The sensitivity analysis leads to the results presented in table 16, which is presented in the same format as table L.2 [5]. In this table column 'm' represents the slope of the two-parameter regression of the bin-wise averaged data. Column 'r^2' represents the correlation coefficient of the two-parameter regression of the scatter data.

For the computation of the bin-wise averages, only those bins are included that meet the following bin-count requirement, stipulated by the criterion in eq. (6.5) [5, eq. L.2]. When the reference wind speed is used as the EV, also the criterion in equation (L.3) needs to be applied.

$$n_i > \frac{N}{2 \cdot n_b} \tag{6.5}$$

The sensitivity, presented in column 'sens.', is defined by

$$\text{sensitivity} = m \cdot \text{std} \tag{6.6}$$

where 'std' is the standard deviation of the EV data.

The sensitivity of the LiDAR for an EV is considered as significant if either the sensitivity exceeds a value of 0.5, or the product of sensitivity and r exceeds 0.1. In table 16, the sensitivity criteria that exceed their threshold value are highlighted in red. The regressions associated with these significant sensitivities are presented in fig. 27. In case a significant sensitivity for an EV is observed for at least one comparison height, that EV must be considered as significant for all comparison heights. Table 14 provides an overview of the significant sensitivities.

6.2 Impact on accuracy

Although our interest is not in determining an accuracy class, but rather investigate the sensitivities presented in section 6.1, we would be amiss not to present the impact these sensitivities have on the accuracy.

The basis for the accuracy class is the product of m, as already presented in table 16, and the range of the EV. The EV ranges are largely prescribed by table L.3 [5]. The

Table 14: Overview of significant sensitivities

environmental variable	comparison height					overall
	100 m	90 m	59 m	44 m	29 m	
shear exponent						
turbulence intensity						
precipitation						
wind direction			✓			✓
air temperature						
relative humidity	✓	✓	✓			✓
air density						
flow inclination						
wind veer						
reference wind speed						

results are presented in table 17, which is presented in a similar format as table L.6 [5]. Because precipitation has only a single bin (0 %) that meets the bin count criterion, no sensitivity can be computed for this EV.

The range is a defined quantity, presented in the column 'range' of table 17. The IEC 61400-12-1 standard defines the measured range of variation through the ratio of bins that meet the criterion in eq. (6.5). The result is presented in the column 'covered range'. The measured range of variation is considered sufficient if the covered range is at least 25 %.

For the relative humidity no range is prescribed; we used 0 % to 100 %. The prescribed flow inclination range of $-3°$ to $3°$ was modified to $-1°$ to $5°$ to better cover the measured range.

The EVs precipitation and air density do not meet the range requirement. For the precipitation this is caused by our choice of the metric: the amount of time precipitation is registered in a 10-minute interval. This causes most samples to fall in either the 0 % or the 100 % bin. For the air density this is caused by the limited variation of air density at the site with respect to the prescribed range.

The last column of table 17 represents the contribution to the preliminary accuracy class for each EV. From this we can draw the conclusion that shear and turbulence have the highest influence on the accuracy.

In order to obtain the preliminary accuracy class, these contributions have to be added in quadrature for each height. The results are presented in table 15, similar to table L.7 [5].

Table 15: Preliminary accuracy classes

height	considering all variables	considering only significant variables
m	-	-
29	7.6	2.9
44	5.6	3.1
59	7.2	4.9
90	7.3	4.9
100	7.6	4.7

It should be noted that the results in table 15 cannot be used directly to derive the final accuracy class numbers, because the interdependency between the EVs has not been eliminated.

Table 16: Parameters derived from the sensitivity analysis of the rsd

height	variable	avg	std	m	sens.	r^2	sens.$\times r$
m	-	unit	unit	1/unit	-	-	-
29	shear exponent	0.227	0.135	3.333	0.452	0.017	0.059
44		0.253	0.149	-1.776	-0.265	0.013	-0.030
59		0.257	0.150	-1.343	-0.201	0.013	-0.023
90		0.258	0.148	-2.839	-0.420	0.038	-0.082
100		0.258	0.147	-3.177	-0.468	0.041	-0.095
29	turbulence intensity	12.753	2.441	0.028	0.067	0.001	0.002
44		9.961	3.492	0.069	0.241	0.011	0.025
59		9.699	3.596	0.049	0.176	0.004	0.011
90		8.206	3.108	0.080	0.250	0.007	0.020
100		8.136	3.086	0.100	0.308	0.010	0.030
29	precipitation	0.042	0.567			0.000	
44		0.035	0.515			0.000	
59		0.033	0.499			0.000	
90		0.033	0.494			0.000	
100		0.027	0.442			0.000	
29	wind direction	203.856	49.753	-0.006	-0.275	0.037	-0.053
44		196.752	52.130	-0.000	-0.026	0.000	-0.000
59		198.703	49.897	-0.008	-0.395	0.077	-0.109
90		197.360	52.327	-0.000	-0.012	0.001	-0.000
100		199.400	47.204	0.002	0.072	0.000	0.001
29	air temperature	17.643	2.032	-0.067	-0.137	0.002	-0.005
44		17.584	2.024	0.006	0.011	0.000	0.000
59		17.638	2.073	0.090	0.186	0.009	0.018
90		17.710	2.141	0.070	0.149	0.000	0.003
100		17.774	2.172	0.054	0.117	0.000	0.001
29	relative humidity	73.118	11.755	-0.028	-0.325	0.012	-0.035
44		72.824	11.414	-0.031	-0.358	0.018	-0.048
59		72.746	11.409	-0.047	-0.537	0.053	-0.123
90		72.467	11.305	-0.049	-0.550	0.029	-0.093
100		72.190	11.368	-0.047	-0.537	0.022	-0.080
29	air density	1.198	0.012	-0.722	-0.009	0.001	-0.000
44		1.199	0.012	3.441	0.041	0.001	0.001
59		1.199	0.012	-1.792	-0.022	0.005	-0.002
90		1.198	0.013	-4.420	-0.058	0.003	-0.003
100		1.198	0.013	-5.774	-0.076	0.002	-0.003
29	flow inclination	1.778	0.708	0.465	0.329	0.023	0.050
44		1.908	0.737	-0.080	-0.059	0.001	-0.002
59		1.934	0.747	0.481	0.359	0.036	0.068
90		1.948	0.749	0.125	0.094	0.002	0.004
100		1.975	0.736	-0.064	-0.047	0.000	-0.000
29	wind veer	-0.043	0.066	-6.400	-0.421	0.027	-0.069
44		-0.050	0.067	2.992	0.202	0.008	0.018
59		-0.052	0.068	-0.608	-0.041	0.002	-0.002
90		-0.054	0.068	2.356	0.161	0.003	0.009
100		-0.054	0.069	3.561	0.244	0.008	0.021

Continued on next page

Table 16 – continued from previous page

height	variable	avg	std	m	sens.	r^2	sens.$\times r$
m	-	unit	unit	1/unit	-	-	-
29	reference wind speed	5.840	1.607	-0.130	-0.209	0.005	-0.014
44		6.009	1.662	0.128	0.213	0.012	0.023
59		6.346	1.744	-0.065	-0.113	0.001	-0.004
90		6.876	1.939	0.054	0.104	0.000	0.002
100		7.114	2.071	0.065	0.135	0.001	0.004

Table 17: Maximum influence of environmental variables on the rsd

height	variable	m	range	covered range	$m\times$ range
m	-	1/unit	unit	%	-
29	shear exponent	3.333	1.20	46	4.000
44		-1.776	1.20	50	-2.131
59		-1.343	1.20	50	-1.612
90		-2.839	1.20	50	-3.406
100		-3.177	1.20	50	-3.813
29	turbulence intensity	0.028	21.00	52	0.578
44		0.069	21.00	67	1.449
59		0.049	21.00	67	1.030
90		0.080	21.00	57	1.687
100		0.100	21.00	57	2.095
29	precipitation		100.00	10	
44			100.00	10	
59			100.00	10	
90			100.00	10	
100			100.00	10	
29	wind direction	-0.006	180.00	49	-0.995
44		-0.000	180.00	54	-0.090
59		-0.008	180.00	53	-1.426
90		-0.000	180.00	53	-0.040
100		0.002	180.00	50	0.275
29	air temperature	-0.067	40.00	30	-2.696
44		0.006	40.00	30	0.226
59		0.090	40.00	30	3.585
90		0.070	40.00	30	2.793
100		0.054	40.00	30	2.148
29	relative humidity	-0.028	100.00	50	-2.767
44		-0.031	100.00	50	-3.135
59		-0.047	100.00	50	-4.706
90		-0.049	100.00	50	-4.865
100		-0.047	100.00	50	-4.727
29	air density	-0.722	0.45	22	-0.325
44		3.441	0.45	22	1.548
59		-1.792	0.45	22	-0.806
90		-4.420	0.45	22	-1.989
100		-5.774	0.45	22	-2.598

Continued on next page

Table 17 – continued from previous page

height	variable	m	range	covered range	$m\times$ range
m	-	1/unit	unit	%	-
29	flow inclination	0.465	6.00	53	2.788
44		-0.080	6.00	57	-0.479
59		0.481	6.00	57	2.888
90		0.125	6.00	57	0.750
100		-0.064	6.00	57	-0.386
29	wind veer	-6.400	0.40	70	-2.560
44		2.992	0.40	70	1.197
59		-0.608	0.40	70	-0.243
90		2.356	0.40	70	0.942
100		3.561	0.40	70	1.424
29	reference wind speed	-0.130	25.00	22	-3.256
44		0.128	25.00	23	3.202
59		-0.065	25.00	25	-1.622
90		0.054	25.00	27	1.342
100		0.065	25.00	28	1.627

7 Uncertainty

This chapter describes the uncertainty contributions to the horizontal wind speed measurement that were taken into account. These uncertainties are the basis for the LiDAR verification analysis reported in chapter 5. The uncertainty analysis is performed for application in the verification analysis only, therefore the uncertainty analysis is limited to the (horizontal) wind speed measurements.

All uncertainties are reported with a coverage factor of one ($k = 1$). To obtain uncertainties for $k = 2$ the results have to be doubled.

7.1 Reference devices - cup anemometers

The following contributions to the systematic uncertainty of the cup anemometers are taken into account in accordance with Annex L.4.2 [5].

1. **Wind tunnel calibration**
   The uncertainty associated with wind tunnel calibration is computed by adding in quadrature the reported (maximum) uncertainty in the wind tunnel speed and the uncertainty due to linearisation.

   The calibration certificate of the Thies First Class Advanced cup anemometer (see section B.1) at the top of the MM4 is used to estimate the uncertainty used for all cup anemometers. The maximum uncertainty in the wind tunnel speed is 0.051 m/s with a coverage factor of two ($k = 2$). The standard error of the regression is 0.005 m/s. The total standard uncertainty therefore is

   $$u_{\text{VS,precal},i} = \sqrt{\left(\frac{0.051\,\text{m/s}}{2}\right)^2 + (0.005\,\text{m/s})^2} = 0.026\,\text{m/s}.$$

2. **Effects according to anemometer classification**
   The classification of the Thies First Class Advanced cup anemometer is 0.9A (for flat terrain). The uncertainty in the wind speed due to operational characteristics therefore is

   $$u_{\text{VS,class},i} = [0.5\,\% + 0.05\,\text{m/s}] \cdot \frac{0.9}{\sqrt{3}}$$

3. **Mounting effects**
   The default values for the uncertainty associated with the mounting of the anemometer on mast are specified in Annex E.6.3.5 [5]. At the height of 100 m two side-by-side top mounted anemometers are used, for which the default uncertainty is

   $$u_{\text{VS,mnt},i} = 1.0\,\%.$$

   At all other comparison heights, side-mounted anemometers are used. Even though at most heights multiple booms are used, so the ‘true wind speed’ pseudo signals allow for a wind speed measurement not obstructed by the mast itself for a wide wind direction sector, this cannot be considered a flow correction. Therefore, for all comparison heights lower than 100 m, the uncertainty magnitude for non-flow-corrected signals is used.

   $$u_{\text{VS,mnt},i} = 1.5\,\%.$$

4. **Data acquisition**
   In accordance with our internal calibration procedure for the Thies frequency

modules [8], the uncertainty of the data acquisition modules based on the measured frequency is estimated as $u_f = 0.429\,\% \cdot f + 0.362\,\text{Hz}$. Table 20 shows that the gains of all Thies cup anemometers are close to 0.046 $\frac{\text{m/s}}{\text{Hz}}$. This results in an uncertainty of the wind speed of

$$u_{\text{dVS},i} = 0.429\,\% + 0.0167\,\text{m/s}.$$

The total systematic uncertainty of the reference sensor is obtained by adding all contributions in quadrature. As in IEC 61400-12-1, this is referred to as 'reference type B' uncertainty in fig. 25.

7.2 Remote sensing device

The following contributions to the uncertainty of the LiDAR wind speed measurements are taken into account in accordance with annex L.4.3 [5].

1. **Systematic uncertainty of the reference sensor**
   This is the systematic uncertainty of the cup anemometer as defined in section 7.1.

2. **Mean deviation**
   No correction of the LiDAR wind speed measurement is performed. Therefore, this contribution is defined as the bin-wise average deviation between the reference sensor and the LiDAR.

3. **Standard uncertainty of the LiDAR measurements**
   The standard uncertainty is defined by eq. (7.1).

$$\text{standard uncertainty}_i = \frac{\sigma_{v_i}}{\sqrt{n_i}} \tag{7.1}$$

   Where σ_{v_i} is the standard deviation of 10-minute average measurements in wind speed bin i and n_i is the bincount.

4. **Mounting effects of the LiDAR**
   We are using the default magnitude stated in clause E.7.5 [5, p.110].

$$u_{\text{VR,mnt},i} = 0.01\,\%$$

   The mounting uncertainty is reported in tables 4 to 8.

5. **Non-homogeneous flow**
   The uncertainty due to non-homogeneous flow in the measurement volume of the LiDAR is estimated from a terrain flow assessment [9] based on the terrain information shown in fig. 4.

$$u_{\text{VR,flow},i} = 0.026\,\%$$

6. **Separation**
   The uncertainty due to the separation between the LiDAR and MM4 is prescribed as

$$u_{\text{VR,sep},i} = 1\,\% \cdot \frac{d_{\text{sep}}}{h}$$

   where d_{sep} is the separation distance between, equal to 5 m, and h is the measurement height of the (reference) wind speed for that comparison height. The uncertainty due to the separation distance is reported in the penultimate column of tables 4 to 8.

The total LiDAR uncertainty is obtained by adding in quadrature the contributions above. The result is reported in the last column of tables 4 to 8. An overview of the various uncertainty contributions is presented in fig. 25.

The uncertainty interval shown in figs. 16 to 20 is also obtained by adding in quadrature the contributions above, but with the exception of the mean deviation.

8 Deviations

Meteorological measurements at MM4 have been performed in accordance with IEC 61400-12-1:2005. No deviations are to be reported in this respect. However Meteorological Mast 4 is not compliant with IEC 61400-12-1:2017.

The LiDAR verification as presented in chapter 5 is performed in accordance with IEC 61400-12-1:2017 Annex L. The following deviation is observed.

The upper bins on the required wind speed range of 4 m/s to 16 m/s are incomplete in all comparison heights.

9 References

[1] C. A. van Diggelen and J. W. Wagenaar. Instrumentation LiDAR Calibration Facility at EWTW. techreport ECN-X--16-119, ECN, August 2016.

[2] Wind turbines - Part 12-1: Power performance measurements of electricity producing wind turbines, December 2005.

[3] Hasager et al. Hub height ocean winds over the North Sea observed by the NORSEWinD lidar array: Measuring techniques, quality control and data management. *Remote Sensing*, 5:4280–4303, 2013.

[4] The Carbon Trust. Carbon Trust Offshore Wind Accelerator roadmap for the commercial acceptance of floating LIDAR technology. techreport CTC819 Version 1.0, The Carbon Trust, November 2013.

[5] Wind energy generation systems - Part 12-1: Power performance measurements of electricity producing wind turbines, March 2017.

[6] P. A. van der Werff. *User manual Meassector 2.2.* ECN, 2015.

[7] I. A. Alting. WDMS4 developer reference. techreport ECN-Wind Memo-11-023, ECN, October 2011.

[8] ECN Wind Energy. Procedure for DANTE Frequency modules, version 4.0. techreport IN-810-033, ECN, 2014.

[9] D. A. J. Wouters. Non-homogeneous flow within a lidar measurement volume at EWTW. techreport TNO 2019 M10109, ECN part of TNO, January 2019.

[10] S. Barhorst and H. Korterink. Meteorological mast 4 at EWTW; instrumentation report. techreport ECN-X--13-087, ECN, December 2013.

10 Signature

	Date: April 2019	**Number of report:** TNO 2018 R10850
Title	Verification of ZephIR 300M unit 563 at ECN part of TNO LiDAR Calibration Facility, for offshore measurements at K13-A production platform	
Author(s)	D.A.J. Wouters and J.P. Verhoef	
Principal(s) Ministry of Economic Affairs Bezuidenhoutseweg 73 2594 AC Den Haag		
ECN project number	5.2241	
Principals' order number	ECN beschikkingsbrief EZ, 2016	
Programme(s)	Wind Energy	

Abstract

As part of the North Sea offshore wind conditions measurement program a ZephIR LiDAR is installed at K13-A production platform on November 2016. In order to assure high quality measurements, the LiDAR unit (ZephIR 300M, 563) was validated at the ECN part of TNO LiDAR Calibration Facility for the period of 31 August 2016 00:00 until 10 October 2016 00:00. ECN part of TNO is ISO 17025 accredited for remote sensing device calibration, where the Meteorological Mast 4 measurements are in accordance with IEC 61400-12-1:2015, Annex G and the LiDAR verification in accordance with IEC 61400-12-1:2017, Annex L. The validation is performed by checking Key Performance Indicators.

Keywords	Verification measurements, ZephIR 300M 563, ECN part of TNO LiDAR Calibration Facility, ELCF, K13-A production platform, K13-A

Authorization	**Name**		**Signature**	**Date**
Checked	J.P. Verhoef	Project manager		2-4-'19
Approved	M. van Roermund	Deputy research manager		2-4-'19
Authorized	M.H. Langelaar	Research manager i.a.		2-4-'19

A IEC visualisations

This appendix contains visualizations associated with the IEC analysis reported in chapters 5 and 6 that are not a reporting requirement.

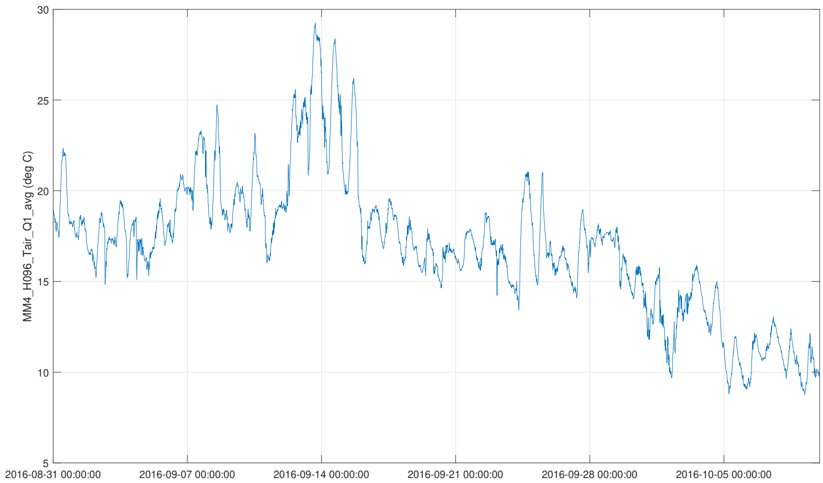

Figure 23: Air temperature @96m

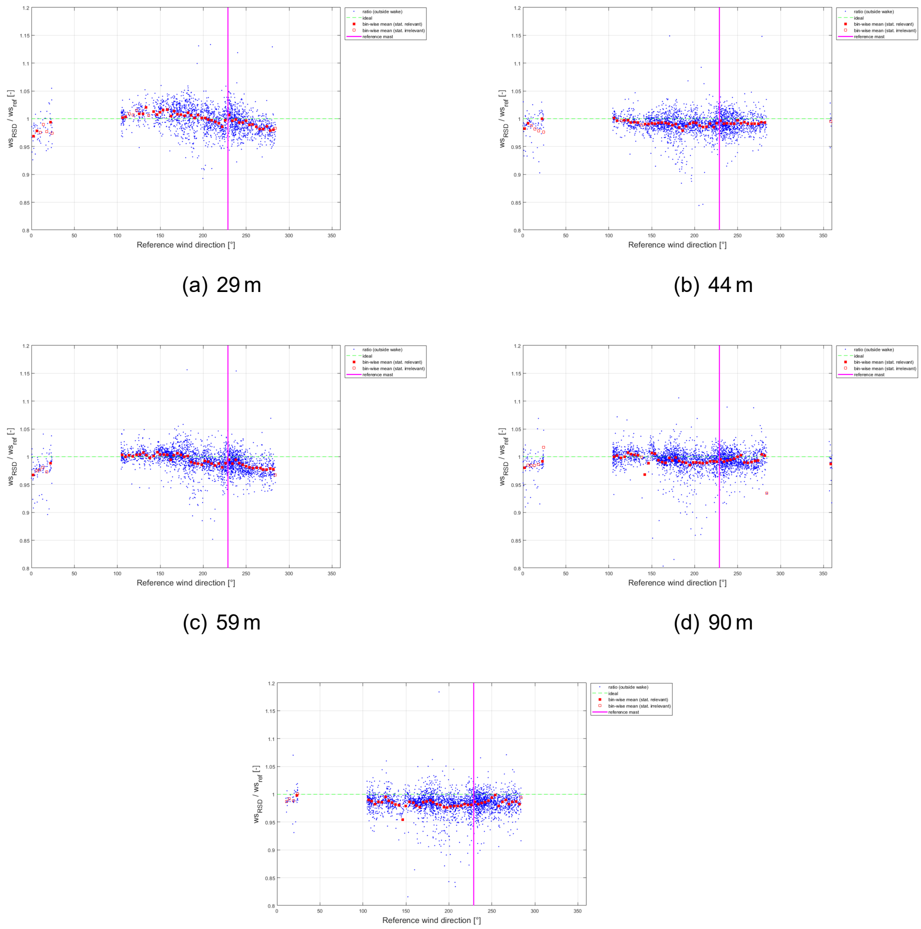

(a) 29 m (b) 44 m

(c) 59 m (d) 90 m

(e) 100 m

Figure 24: Influence of the wake of MM4 on the LiDAR

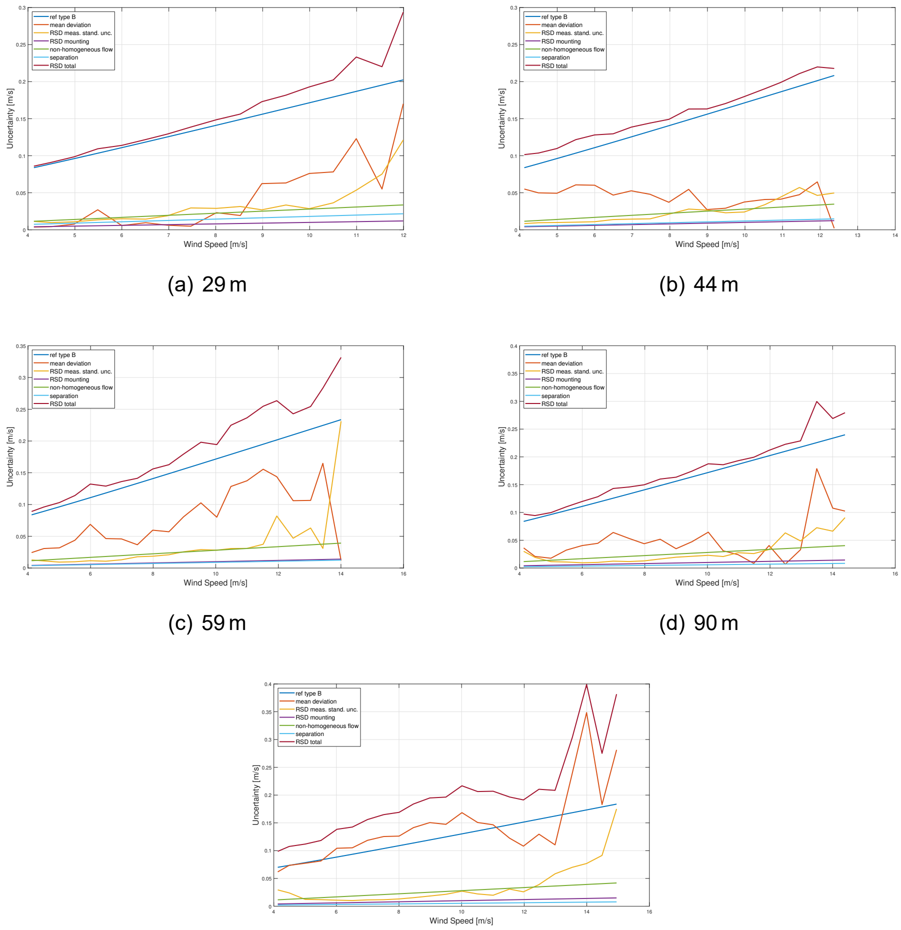

(a) 29 m (b) 44 m

(c) 59 m (d) 90 m

(e) 100 m

Figure 25: Contributions to the LiDAR uncertainty

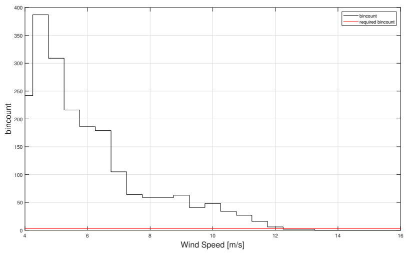

(a) 29 m

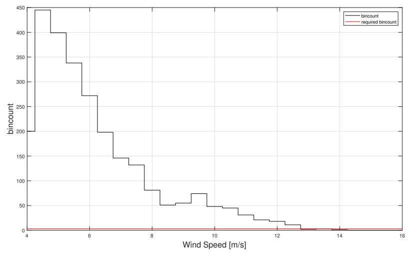

(b) 44 m

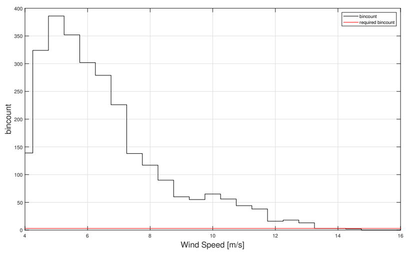

(c) 59 m

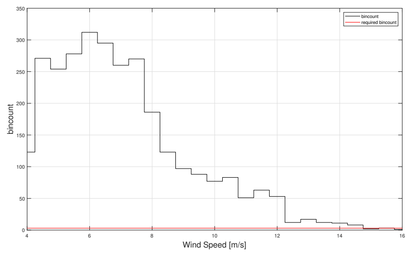

(d) 90 m

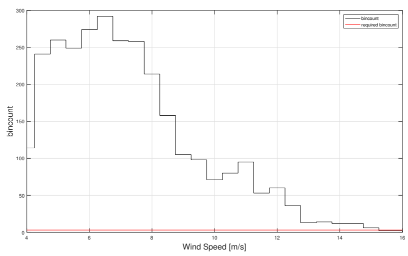

(e) 100 m

Figure 26: Histograms for bin-wise wind speed comparison

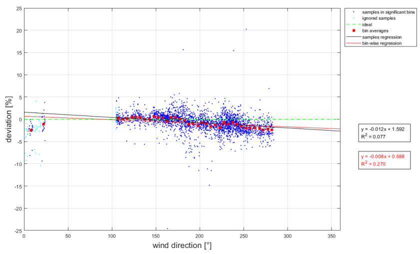

(a) wind direction @59 m

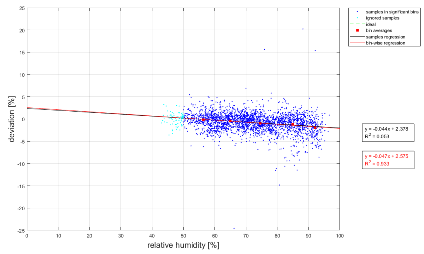

(b) relative humidity @59 m

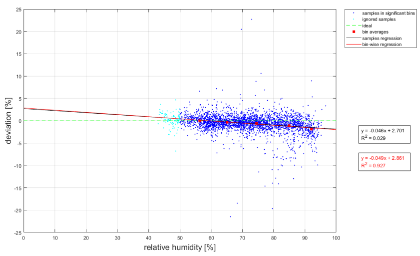

(c) relative humidity @90 m

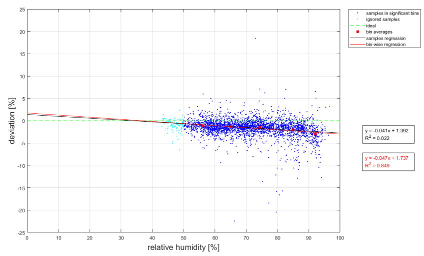

(d) relative humidity @100 m

Figure 27: Significant LiDAR sensitivities

B Instrumentation details

This appendix presents the instrumentation details of the Meteorological Mast 4 and the LiDAR.

Figure 28 presents a schematic overview of the layout of the mast. The mast is described in more detail in the Meteorological Mast 4 instrumentation report [10].

The heights presented in fig. 28 refer to the heights of the booms. Table 18 uses the heights of the sensors of the metmast. At these heights the metmast measurements are compared to the LiDAR measurements. Table 18 lists these comparison heights and the wind speed and wind direction signals used from both MM4 and the LiDAR. All of these signals are 10-minute average statistics.

Some of these statistics are directly derived from measured signals, which are presented in the instrumentation list in table 19. Other statistics are based on pseudo signals, which are listed in table 21.

The sensors used to measure these signals and the data acquisition modules they are attached to are listed in table table 20. This table also presents installation and calibration due dates.

Table 18: Signals used for each comparison heights

height	metmast	LiDAR
m		
	wind speed	
100	MM4_H100_Ws_True_Q1_avg	Z563S_H99_WsHor_avg
90	MM4_H090_Ws_True_Q1_avg	Z563S_H89_WsHor_avg
59	MM4_H059B155_Ws_Q1_avg	Z563S_H58_WsHor_avg
44	MM4_H044_Ws_True_Q1_avg	Z563S_H43_WsHor_avg
29	MM4_H029B155_Ws_Q1_avg	Z563S_H28_WsHor_avg
	wind direction	
100	MM4_H097_Wd_True_Q1_avg	Z563S_H99_Wd
90	MM4_H088_Wd_True_Q1_avg	Z563S_H89_Wd
59	MM4_H057B155_Wd_Q1_avg	Z563S_H58_Wd
44	MM4_H042_Wd_True_Q1_avg	Z563S_H43_Wd
29	MM4_H027B155_Wd_Q1_avg	Z563S_H28_Wd

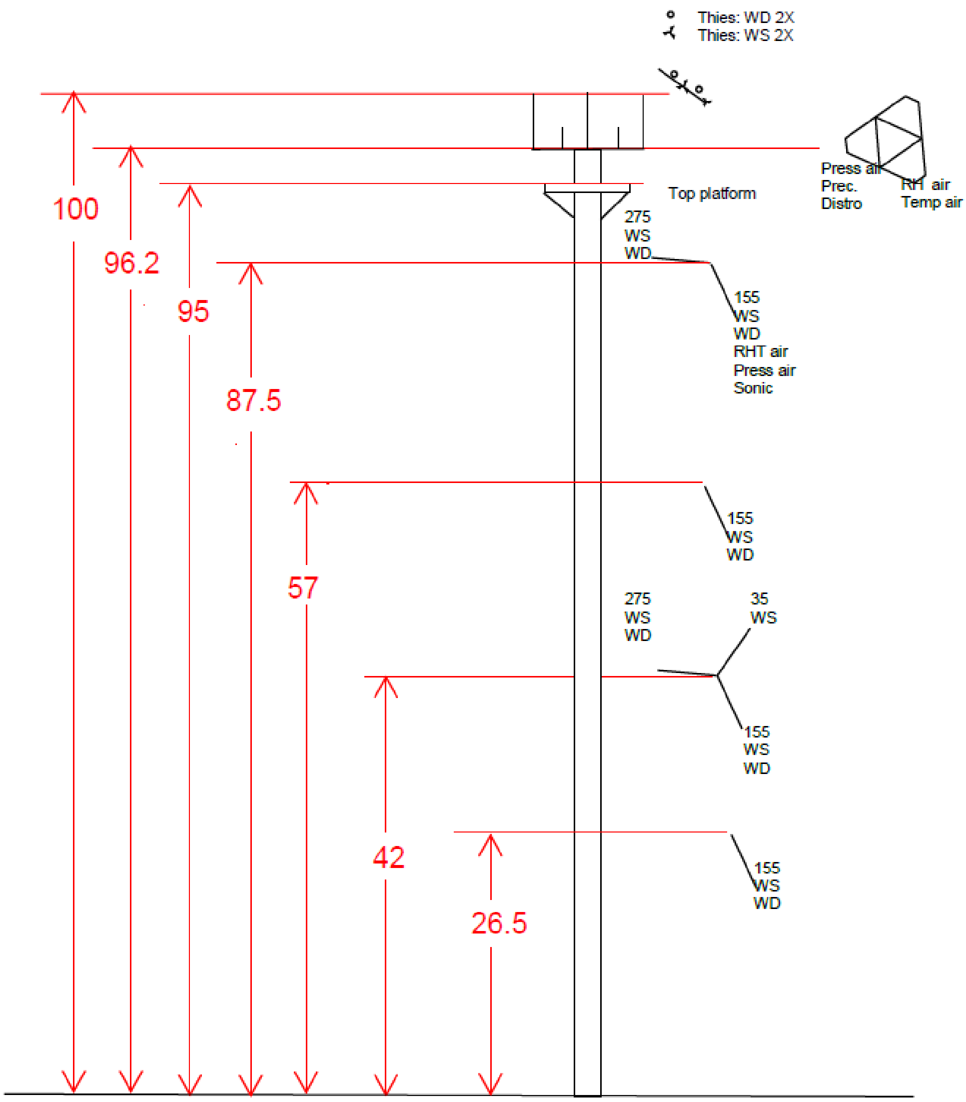

Source: ECN-X--13-087 [10]

Figure 28: Layout of Meteorological Mast 4

Table 19: List of measured signals

name	location	short name	sensor	unit	installed	rate	ISO
						Hz	
wind speed, 100 m, centre	MM4	MM4_H100B000_Ws_Q1_m	Thies First class Advanced cup anemometer	m/s	ECN	4	*
wind speed, 100 m, 305°	MM4	MM4_H100B305_Ws_Q1_m	Thies First class Advanced cup anemometer	m/s	ECN	4	*
wind speed, 90 m, 155°	MM4	MM4_H090B155_Ws_Q1_m	First class Advanced cup anemometer	m/s	ECN	4	*
wind speed, 90 m, 275°	MM4	MM4_H090B275_Ws_Q1_m	First class Advanced cup anemometer	m/s	ECN	4	*
wind speed, 59 m, 155°	MM4	MM4_H059B155_Ws_Q1_m	First class Advanced cup anemometer	m/s	ECN	4	*
wind speed, 44 m, 35°	MM4	MM4_H044B035_Ws_Q1_m	First class Advanced cup anemometer	m/s	ECN	4	*
wind speed, 44 m, 155°	MM4	MM4_H044B155_Ws_Q1_m	First class Advanced cup anemometer	m/s	ECN	4	*
wind speed, 44 m, 275°	MM4	MM4_H044B275_Ws_Q1_m	First class Advanced cup anemometer	m/s	ECN	4	*
wind speed, 29 m, 155°	MM4	MM4_H044B155_Ws_Q1_m	First class Advanced cup anemometer	m/s	ECN	4	*
wind direction, 97 m, 125°	MM4	MM4_H097B125_Wd_Q1_m	First class wind vane	°	ECN	4	*
wind direction, 97 m, 305°	MM4	MM4_H097B305_Wd_Q1_m	First class wind vane	°	ECN	4	*
wind direction, 88 m, 155°	MM4	MM4_H088B155_Wd_Q1_m	First class wind vane	°	ECN	4	*
wind direction, 88 m, 275°	MM4	MM4_H088B275_Wd_Q1_m	First class wind vane	°	ECN	4	*
wind direction, 57 m, 155°	MM4	MM4_H057B155_Wd_Q1_m	First class wind vane	°	ECN	4	*
wind direction, 42 m, 155°	MM4	MM4_H042B155_Wd_Q1_m	First class wind vane	°	ECN	4	*
wind direction, 42 m, 275°	MM4	MM4_H042B275_Wd_Q1_m	First class wind vane	°	ECN	4	*
wind direction, 27 m, 155°	MM4	MM4_H027B155_Wd_Q1_m	First class wind vane	°	ECN	4	*
air temperature, 96 m	MM4	MM4_H096_TempAir_Q1_m	temperature probe	°C	ECN	4	*
relative humidity, 96 m	MM4	MM4_H096_RH_Q1_m	humidity probe	%	ECN	4	*
air pressure, 96 m	MM4	MM4_H096_Pair_Q1_m	digital barometer	hPa	ECN	4	*
precipitation, distro, 96 m	MM4	MM4_H096_Prec_Distro_Q1_m	laser precipitation monitor	%	ECN	1	*
wind speed, sonic u, 87 m, 155°	MM4	MM4_H087B155_S_U_Q5_m	ultrasonic anemometer	m/s	ECN	4	
wind speed, sonic v, 87 m, 155°	MM4	MM4_H087B155_S_V_Q5_m	ultrasonic anemometer	m/s	ECN	4	
wind speed, sonic w, 87 m, 155°	MM4	MM4_H087B155_S_W_Q5_m	ultrasonic anemometer	m/s	ECN	4	

Table 20: List of equipment used per signal

Signal	Sensor						Modue				
short name	brand / type	ID	gain	offset[a]	cal. due date[b]	inst. date	type	ID	gain	offset	cal. due date
MM4_H100B000_Ws_Q1_m	Thies 4.3351.00.000	1926	4.600e-2	2.302e-1	2017-03-31	2016-03-31	frequency 0-1 kHz	2089	2.4445e-1	1.8276e+0	2017-08-02
MM4_H100B305_Ws_Q1_m	Thies 4.3351.00.000	2184	4.611e-2	2.179e-1	2017-03-31	2016-03-31	frequency 0-1 kHz	2090	2.4562e-1	8.8240e-1	2017-08-02
MM4_H090B155_Ws_Q1_m	Thies 4.3351.00.000	5189	4.583e-2	2.399e-1	2016-10-27	2015-10-27	frequency 0-1 kHz	0753	2.4596e-1	9.7057e-1	2017-08-02
MM4_H090B275_Ws_Q1_m	Thies 4.3351.00.000	5187	4.594e-2	2.267e-1	2016-10-27	2015-10-27	frequency 0-1 kHz	5164	2.4549e-1	1.0387e+0	2017-08-02
MM4_H059B155_Ws_Q1_m	Thies 4.3351.00.000	5188	4.590e-2	2.244e-1	2016-10-27	2015-10-27	frequency 0-1 kHz	5163	2.4452e-1	1.4630e+0	2017-08-02
MM4_H044B035_Ws_Q1_m	Thies 4.3351.00.000	1979	4.607e-2	2.249e-1	2017-03-31	2016-03-31	frequency 0-1 kHz	2027	2.4435e-1	1.5767e+0	2017-08-02
MM4_H044B155_Ws_Q1_m	Thies 4.3351.00.000	2104	4.593e-2	2.316e-1	2017-03-31	2016-03-31	frequency 0-1 kHz	2028	2.4480e-1	1.4008e+0	2017-08-02
MM4_H044B275_Ws_Q1_m	Thies 4.3351.00.000	2105	4.597e-2	2.393e-1	2017-03-31	2016-03-31	frequency 0-1 kHz	2086	2.4591e-1	1.3413e+0	2017-08-02
MM4_H029B155_Ws_Q1_m	Thies 4.3351.00.000	5198	4.595e-2	2.318e-1	2016-10-27	2015-10-27	frequency 0-1 kHz	1990	2.4468e-1	1.3978e+0	2017-08-02
MM4_H097B125_Wd_Q1_m	Thies 4.3150.00.400	5124	1.000e-1	6.350e+1	2017-03-31	2016-03-31	RS485 Thies module	5133	1.0000e+0	0.0000e+0	2021-02-24
MM4_H097B305_Wd_Q1_m	Thies 4.3150.00.400	5112	1.000e-1	-1.570e+1	2017-03-31	2016-03-31	RS485 Thies module	1933	1.0000e+0	0.0000e+0	2021-02-24
MM4_H088B155_Wd_Q1_m	Thies 4.3150.00.400	2214	1.000e-1	-7.140e+1	2017-02-25	2016-02-25	RS485 Thies module	5234	1.0000e+0	0.0000e+0	2018-07-02
MM4_H088B275_Wd_Q1_m	Thies 4.3150.00.400	5191	1.000e-1	5.500e+0	2016-10-27	2015-10-27	RS485 Thies module	5226	1.0000e+0	0.0000e+0	2018-07-02
MM4_H057B155_Wd_Q1_m	Thies 4.3150.00.400	5114	1.000e-1	-3.670e+1	2016-10-27	2015-10-27	RS485 Thies module	5227	1.0000e+0	0.0000e+0	2018-07-02
MM4_H042B155_Wd_Q1_m	Thies 4.3150.00.400	2172	1.000e-1	-2.010e+1	2017-03-31	2016-03-31	RS485 Thies module	5131	1.0000e+0	0.0000e+0	2021-02-24
MM4_H042B275_Wd_Q1_m	Thies 4.3150.00.400	5115	1.000e-1	1.050e+1	2017-03-31	2016-03-31	RS485 Thies module	5132	1.0000e+0	0.0000e+0	2021-02-24
MM4_H027B155_Wd_Q1_m	Thies 4.3150.00.000	5190	1.000e-1	-1.070e+1	2016-10-27	2015-10-27	RS485 Thies module	5228	1.0000e+0	0.0000e+0	2018-07-02
MM4_H096_TempAir_Q1_m MM4_H096_RH_Q1_m	Vaisala HMP155	2265	1.000e-1	0.000e+0	2017-03-21	2016-03-31	RS422 Vaisala RH-T 2ch module	5134	1.0000e+0	0.0000e+0	2021-02-24
MM4_H096_Pair_Q1_m	Vaisala PTB210	6078	1.000e+0	0.000e+0	2017-03-21	2016-03-31	RS485 PTB210 module	5197	1.0000e-2	7.5000e+2	2021-08-02
MM4_H096_Prec_Distro_Q1_m	Thies 5.4110.00.000	5130	1.000e+2	0.000e+0	none	2013-01-07	RS485 distro module	5202	1.0000e+0	0.0000e+0	2021-07-03
MM4_H087B155_S_U_Q5_m MM4_H087B155_S_V_Q5_m MM4_H087B155_S_W_Q5_m	Metek USA-1	2244	1.000e-2	0.000e+0	2019-10-29	2014-11-28	RS422 Metek USA1 3D Sonic Head Corr module	5229	1.0000e+0	0.0000e+0	2023-07-04

a]For wind vanes the offset is governed by the North alignment of the vane w.r.t. its mounting orientation. Hence it does not reflect the offset reported on the calibration certificate.
b]For cup anemometers and wind vanes the (annual) calibration due date is based on the installation date (not the wind tunnel calibration date).

Table 21: List of calculated (pseudo) signals

name	short name	unit	rate	ISO	constituents/derivation	
			Hz			
wind speed, 100 m	MM4_H100_Ws_True_Q1	m/s	4	*	MM4_H097_Wd_True_Q1 MM4_H100B000_Ws_Q1_m MM4_H100B305_Ws_Q1_m	B.1
wind speed, 90 m	MM4_H090_Ws_True_Q1	m/s	4	*	MM4_H088_Wd_True_Q1 MM4_H090B155_Ws_Q1_m MM4_H090B275_Ws_Q1_m	B.2
wind speed, 44 m	MM4_H044_Ws_True_Q1	m/s	4	*	MM4_H042_Wd_True_Q1 MM4_H044B035_Ws_Q1_m MM4_H044B155_Ws_Q1_m MM4_H044B275_Ws_Q1_m	B.3
wind direction, 97 m	MM4_H097_Wd_True_Q1	°	4	*	MM4_H097B125_Wd_Q1_m MM4_H097B305_Wd_Q1_m	B.4
wind direction, 88 m	MM4_H088_Wd_True_Q1	°	4	*	MM4_H088B155_Wd_Q1_m MM4_H088B275_Wd_Q1_m	B.5
wind direction, 42 m	MM4_H042_Wd_True_Q1	°	4	*	MM4_H042B155_Wd_Q1_m MM4_H042B275_Wd_Q1_m	B.5
horizontal wind speed, sonic, 87 m	MM4_H087B155_Sonic_WsHor_Q5	m/s	4		MM4_H087B155_S_U_Q5_m MM4_H087B155_S_V_Q5_m	B.6

$$f(\#1,\#2,\#3) = \begin{cases} \#2, & \text{if } 35° < \#1 \leq 215° \\ \#3, & \text{otherwise} \end{cases} \tag{B.1}$$

$$f(\#1,\#2,\#3) = \begin{cases} \#2, & \text{if } 35° \leq \#1 < 155° \\ \frac{\#2+\#3}{2}, & \text{if } 155° \leq \#1 < 275° \\ \#3, & \text{otherwise} \end{cases} \tag{B.2}$$

$$f(\#1,\#2,\#3,\#4) = \begin{cases} \frac{\#2+\#3}{2}, & \text{if } 35° \leq \#1 < 155° \\ \frac{\#3+\#4}{2}, & \text{if } 155° \leq \#1 < 275° \\ \frac{\#2+\#4}{2}, & \text{otherwise} \end{cases} \tag{B.3}$$

$$f(\#1,\#2) = \begin{cases} \#1, & \text{if } 95° < \#1 \leq 215° \\ \#2, & \text{if } 215° < \#2 \leq 335° \\ \frac{\#1+\#2}{2}, & \text{otherwise} \end{cases} \tag{B.4}$$

$$f(\#1,\#2) = \begin{cases} \#1, & \text{if } 35° < \#1 < 140° \vee 215° < \#1 < 290° \\ \#2, & \text{otherwise} \end{cases} \tag{B.5}$$

$$f(\#1,\#2) = \sqrt{\#1^2 + \#2^2} \tag{B.6}$$

B.1 Calibration sheets

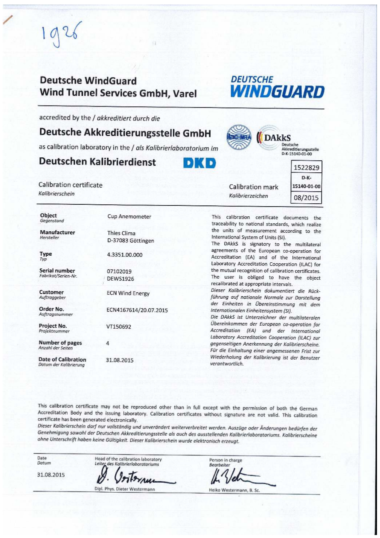

1926

Deutsche WindGuard
Wind Tunnel Services GmbH, Varel

DEUTSCHE WINDGUARD

accredited by the / *akkreditiert durch die*
Deutsche Akkreditierungsstelle GmbH
as calibration laboratory in the / *als Kalibrierlaboratorium im*
Deutschen Kalibrierdienst DKD

DAkkS Deutsche Akkreditierungsstelle D-K-15140-01-00

Calibration certificate / *Kalibrierschein*

Calibration mark / *Kalibrierzeichen*: 1522829 D-K-15140-01-00 08/2015

Object *Gegenstand*	Cup Anemometer
Manufacturer *Hersteller*	Thies Clima D-37083 Göttingen
Type *Typ*	4.3351.00.000
Serial number *Fabrikat/Serien-Nr.*	07102019 DEWS1926
Customer *Auftraggeber*	ECN Wind Energy
Order No. *Auftragsnummer*	ECN4167614/20.07.2015
Project No. *Projektnummer*	VT150692
Number of pages *Anzahl der Seiten*	4
Date of Calibration *Datum der Kalibrierung*	31.08.2015

This calibration certificate documents the traceability to national standards, which realize the units of measurement according to the International System of Units (SI).
The DAkkS is signatory to the multilateral agreements of the European co-operation for Accreditation (EA) and of the International Laboratory Accreditation Cooperation (ILAC) for the mutual recognition of calibration certificates.
The user is obliged to have the object recalibrated at appropriate intervals.
Dieser Kalibrierschein dokumentiert die Rückführung auf nationale Normale zur Darstellung der Einheiten in Übereinstimmung mit dem Internationalen Einheitensystem (SI).
Die DAkkS ist Unterzeichner der multilateralen Übereinkommen der European co-operation for Accreditation (EA) und der International Laboratory Accreditation Cooperation (ILAC) zur gegenseitigen Anerkennung der Kalibrierscheine.
Für die Einhaltung einer angemessenen Frist zur Wiederholung der Kalibrierung ist der Benutzer verantwortlich.

This calibration certificate may not be reproduced other than in full except with the permission of both the German Accreditation Body and the issuing laboratory. Calibration certificates without signature are not valid. This calibration certificate has been generated electronically.
Dieser Kalibrierschein darf nur vollständig und unverändert weiterverbreitet werden. Auszüge oder Änderungen bedürfen der Genehmigung sowohl der Deutschen Akkreditierungsstelle als auch des ausstellenden Kalibrierlaboratoriums. Kalibrierscheine ohne Unterschrift haben keine Gültigkeit. Dieser Kalibrierschein wurde elektronisch erzeugt.

Date / *Datum*: 31.08.2015
Head of the calibration laboratory / *Leiter des Kalibrierlaboratoriums*: Dipl. Phys. Dieter Westermann
Person in charge / *Bearbeiter*: Heiko Westermann, B. Sc.

(a) Cup anemometer 1926, page 1/4

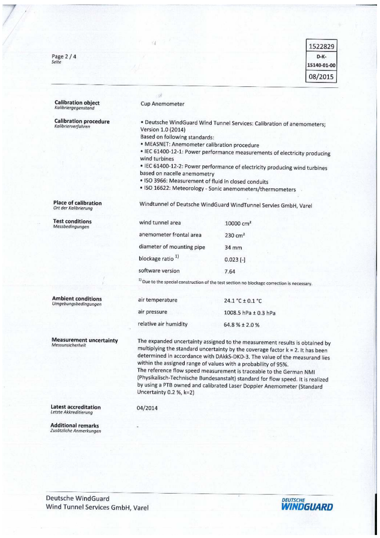

Page 2 / 4 *Seite*

1522829 D-K-15140-01-00 08/2015

Calibration object *Kalibriergegenstand*: Cup Anemometer

Calibration procedure *Kalibrierverfahren*:
- Deutsche WindGuard Wind Tunnel Services: Calibration of anemometers; Version 1.0 (2014)

Based on following standards:
- MEASNET: Anemometer calibration procedure
- IEC 61400-12-1: Power performance measurements of electricity producing wind turbines
- IEC 61400-12-2: Power performance of electricity producing wind turbines based on nacelle anemometry
- ISO 3966: Measurement of fluid in closed conduits
- ISO 16622: Meteorology - Sonic anemometers/thermometers

Place of calibration *Ort der Kalibrierung*: Windtunnel of Deutsche WindGuard WindTunnel Servies GmbH, Varel

Test conditions *Messbedingungen*:

wind tunnel area	10000 cm²
anemometer frontal area	230 cm²
diameter of mounting pipe	34 mm
blockage ratio [1)]	0.023 [-]
software version	7.64

[1)] Due to the special construction of the test section no blockage correction is necessary.

Ambient conditions *Umgebungsbedingungen*:

air temperature	24.1 °C ± 0.1 °C
air pressure	1008.5 hPa ± 0.3 hPa
relative air humidity	64.8 % ± 2.0 %

Measurement uncertainty *Messunsicherheit*: The expanded uncertainty assigned to the measurement results is obtained by multiplying the standard uncertainty by the coverage factor k = 2. It has been determined in accordance with DAkkS-DKD-3. The value of the measurand lies within the assigned range of values with a probability of 95%.
The reference flow speed measurement is traceable to the German NMI (Physikalisch-Technische Bundesanstalt) standard for flow speed. It is realized by using a PTB owned and calibrated Laser Doppler Anemometer (Standard Uncertainty 0.2 %, k=2)

Latest accreditation *Letzte Akkreditierung*: 04/2014

Additional remarks *Zusätzliche Anmerkungen*: -

Deutsche WindGuard
Wind Tunnel Services GmbH, Varel

DEUTSCHE WINDGUARD

(b) Cup anemometer 1926, page 2/4

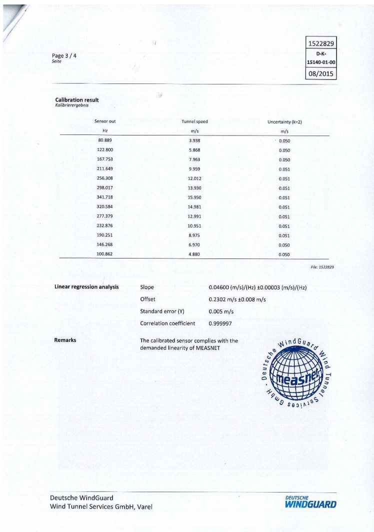

Page 3 / 4 *Seite*

1522829 D-K-15140-01-00 08/2015

Calibration result *Kalibrierergebnis*

Sensor out Hz	Tunnel speed m/s	Uncertainty (k=2) m/s
80.889	3.938	0.050
122.800	5.868	0.050
167.753	7.963	0.050
211.649	9.959	0.051
256.308	12.012	0.051
298.017	13.930	0.051
341.718	15.950	0.051
320.584	14.981	0.051
277.379	12.991	0.051
232.876	10.951	0.051
190.251	8.975	0.051
146.268	6.970	0.050
100.862	4.880	0.050

File: 1522829

Linear regression analysis

Slope	0.04600 (m/s)/(Hz) ±0.00003 (m/s)/(Hz)
Offset	0.2302 m/s ±0.008 m/s
Standard error (Y)	0.005 m/s
Correlation coefficient	0.999997

Remarks: The calibrated sensor complies with the demanded linearity of MEASNET

Deutsche WindGuard Wind Tunnel Services GmbH - measnet

Deutsche WindGuard
Wind Tunnel Services GmbH, Varel

DEUTSCHE WINDGUARD

(c) Cup anemometer 1926, page 3/4

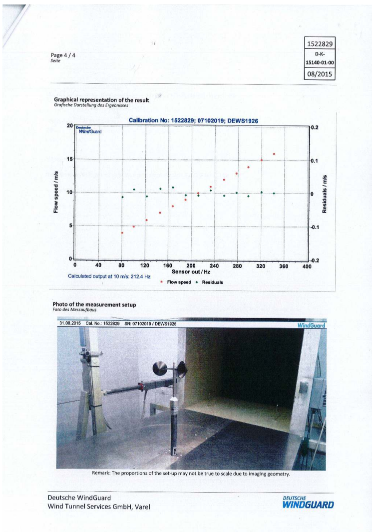

(d) Cup anemometer 1926, page 4/4

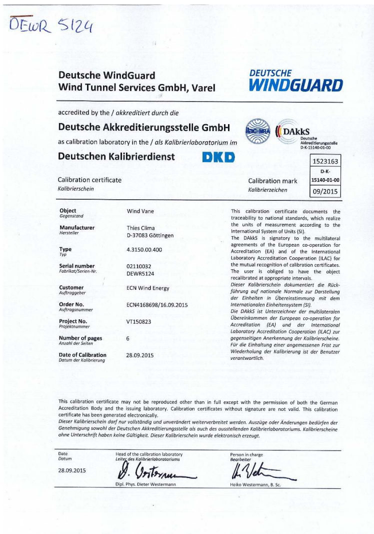

(e) Wind vane 5124, page 1/6

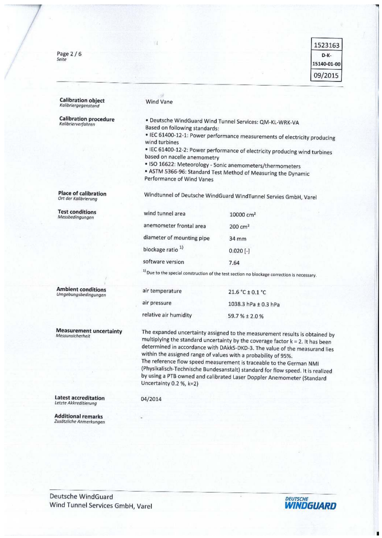

(f) Wind vane 5124, page 2/6

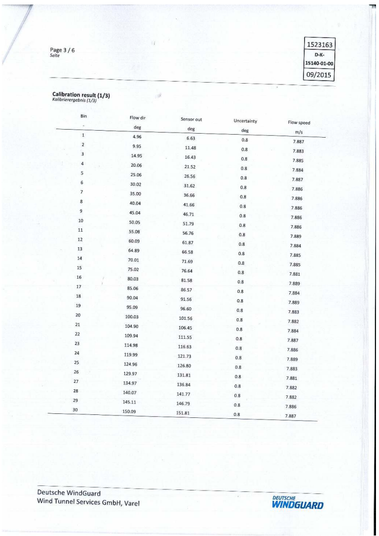

(g) Wind vane 5124, page 3/6

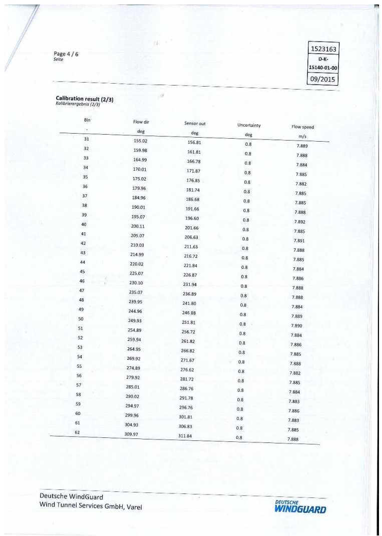

(h) Wind vane 5124, page 4/6

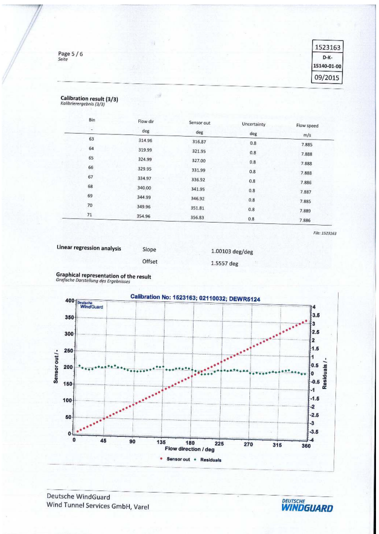

(i) Wind vane 5124, page 5/6

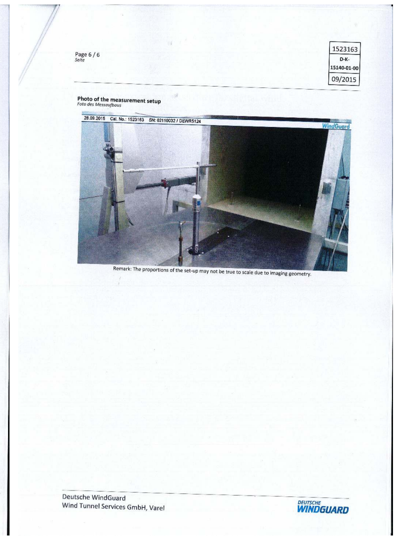

(j) Wind vane 5124, page 6/6

Nomenclature

α	exponent of the power law wind shear model, see equation (6.1)
AHN	Actueel Hoogtebestand Nederland
DTM	Digital Terrain Model
ELCF	ECN part of TNO LiDAR Calibration Facility
EPL	Euro Platform
EV	environmental variable
EWTW	ECN Wind Turbine test site Wieringermeer
h	measurement height, see equation (6.1)
h_r	reference height for shear profile, see equation (6.1)
IEC	International Electrotechnical Commission
ILAC MRA	International Laboratory Accreditation Cooperation Mutual Recognition Arrangement[2]
LEG	Lichteiland Goeree
MPDA	monthly post-processed data availability
MSA	monthly system availability
N	number of 10-minute samples, see equation (6.5)
n_b	number of bins, see equation (6.5)
n_i	bin-count for bin i, see equation (6.5)
OWA	Offshore Wind Accelerator
PDOK	Publieke Dienstvoorziening Op de Kaart
RD	Rijksdriehoekscoördinaten
ref	reference device for comparison, i.e. the metmast
rsd	remote sensing device
RvA	Raad voor Accreditatie[3] / Dutch Accreditation Council
std	standard deviation
UTC	Coordinated Universal Time
v_d	wind direction, see equation (6.4)
v_{hor}	horizontal wind speed, see equation (6.3)
v_r	wind speed of shear profile at h_r, see equation (6.1)
v_{ref}	10-minute average wind speed measured by the ref, see equation (4.1)
v_{rsd}	10-minute average wind speed measured by the rsd, see equation (4.1)
v_{vert}	vertical wind speed, see equation (6.3)
WDMS	Wind Data Management System

[2] `https://ilac.org/signatory-detail/?id=47`

[3] `https://www.rva.nl/en/scopes/details/L324`